Impact of biochar on the metabolic networks of a PHE-degrading microbial community and its influencing mechanism on soil biogeochemical cycles

Dapeng Li
Northeast Agricultural University
Xianyue Li
Northeast Agricultural University
Qiuying Song
Northeast Agricultural University
Qiquan Wang
Northeast Agricultural University
Xinxin Jiang
Northeast Agricultural University
Long Tang
Xi'an Jiaotong University
Yang Gao
Xi'an University of Technology
Xinyue Zhao
Northeast Agricultural University
Hailian Zang
Northeast Agricultural University
Wei Zhao
Northeast Agricultural University
Chunyan Li
Northeast Agricultural University
Ning Hou (houning@neau.edu.cn)
Northeast Agricultural University https://orcid.org/0000-0001-6707-7887

Research

Keywords: Biochar, Bacterial inoculant, PAHs, Contaminated soil remediation, Metagenomics, Biogeochemical cycle

Posted Date: August 18th, 2020

DOI: https://doi.org/10.21203/rs.3.rs-59562/v1

Abstract

Background: Straw pyrolysis into biochar are beneficial for resource recovery and soil improvement. However, little is known about how biochar influences polycyclic aromatic hydrocarbons (PAHs) metabolic pathways and biogeochemical cycles in PAH-contaminated agricultural soil. Here we assessed the influence of biochar and bacterial inoculant on the soil physicochemical properties, the microorganisms involved in the metabolism of PAH and C, N, P and S cycling.

Results: The addition of biochar and bacterial inoculant improved soil fertility and crop nutrition. The community metabolism of phenanthrene was revealed by modeling a gene network based on shotgun metagenomes. Biochar addition in soil promoted the abundance of various phenanthrene-degrading microorganisms involved in multiple steps of phenanthrene catabolism, thereby promoting phenanthrene degradation. Meanwhile, biochar addition increased nitrate reduction and degradation of relatively easily decomposable organic carbon, including cellulose, but it also inhibited lignin and chitin degradation and C and N fixation, while the addition of bacterial inoculant partially mitigated biochar's inhibitory effects in element cycle and inhibited N_2O emission, which alleviated the greenhouse effect.

Conclusions: When bioremediating PAH-contaminated soil, recommendation is to use biochar combined with functional microorganism. This work contributes to expand the current knowledge of the treatment of contaminated soil and provide some empirical evidence for the treatment of contaminated soil by biochar and bacterial inoculant.

1 Background

Biochar is the product of limited oxygen pyrolysis of biomass and is used in agriculture as a soil improver, compost additive and livestock feed supplement [1–4].Some studies have investigated whether biochar not only provides space for soil microorganisms with pore structures but also provides nutrients to soil microorganisms to enhance their growth, and these nutrients are adsorbed on the biochar [5, 6]. In this way, biochar will positively affect soil microbes, thereby accelerating the biodegradation of organic contaminants in soil. Studies have indicated that the effects of biochar on soil microbes and the dissipation of polycyclic aromatic hydrocarbons (PAHs) are significant [7–9]. As a kind of persistent environmental contaminant, PAHs can be efficiently degraded by microbes [10, 11]. Microorganisms using PAHs as carbon sources play a vital role in natural pollutant attenuation in polluted ecosystems [12, 13]. In fact, PAH degradation by mixed microbial communities requires various microbial coordination [14, 15]. However, we still lack a comprehensive view of the principal microbial actors of PAH degradation and their metabolic network in contaminated soils, especially in terms of how PAH degradation is altered by the presence of biochar.

As a kind of soil amendment, the use of biochar with functional microorganisms to treat contaminated soil will not only affect organic contaminant degradation and catabolic pathways but also affect the global biogeochemical cycles of nutrient elements [1, 16]. Studies have found that biochar produced via pyrolysis of biomass wastes can enhance and supply long-term soil organic carbon storage [17, 18]. Nitrogen, the most important nutrient in the ecosystem, is a necessary part of biological organisms and nucleic acids; additionally, nitrogen often represents a limiting factor that restricts the net primary production of ecosystems [19]. Evidence suggests that biochar addition can arouse cardinal changes in soil nutrient cycles, usually leading to crop yield increases, especially in acidic and sterile soils with low soil organic matter content, despite the comparable results in temperate soils that are mutable [20, 21]. However, although these insights into the role of biochar in ecosystems exist, a detailed understanding of how biochar affects the global biogeochemical cycles of nutrient elements is still lacking. Research on how biochar affects the phosphorus (P) and sulfur (S) cycles of organic contaminated soil is lacking, but several microorganisms are related to the process of circulation, and changes in the cycles will change the existence of P and S in the soil, thereby affecting the soil ecological environment. It is unclear how biochar can affect the cycling processes of carbon (C), nitrogen (N), P, and S in organically contaminated soils and whether biochar can improve the soil environment and ecosystems when remediating contaminated soil. The answers to these questions are critical for determining the ability of biochar to repair soil.

Our study aims to provide insights into the impact of the addition of biochar and PAH-degrading bacterial inoculant on the metabolic networks of a PAH-degrading microbial community. We also wanted to provide a detailed mechanistic understanding of how biochar influences the global biogeochemical cycles of the basic nutrient elements (C, N, P, S) in soil.

2 Materials And Methods

2.1 Raw material

The rice straw used in this study came from rural areas located around Yilan County, Hei Longjiang Province, China (46°19'22.79"N, 129°33'40.24"E). The straw was dried to a constant weight at 80°C and then crushed at 25 000 rpm before pyrolysis. The obtained straw powders were stored in a desiccator. The seeds used in this study were collected from the Liyuan seed shop; the seed was a perennial ryegrass seed, which is a high-quality grass species with a high germination rate.

The soil was collected from the cultivated layer of the experimental field (45°44'31.44"N, 126°43'14.00"E) located at Northeast Agricultural University, Heilongjiang Province, China. After the soil reached the laboratory, it passed a 2-mm sieve and was air-dried before the experiment. The obtained soil was stored at room temperature. The soil physicochemical properties were as follows: 1.12 mg kg^{-1} total nitrogen (N), 0.96 mg kg^{-1} total phosphorus (P), 20.8 mg kg^{-1} total potassium (K), 37.9 mg kg^{-1} organic matter, and pH 7.40. For spiking, phenanthrene (PHE) at 300 mg kg^{-1} was applied to the soil. PHE standards (98.7% purity) were purchased from Sigma-Aldrich (America). We mixed 1 kg dry soil with 60 mL of the PHE stock solutions (50 mg mL^{-1} in

acetone). After the solvent had completely evaporated (in a fume hood for 48 h), an aliquot of 0.8 kg contaminated soil was mixed with 7.2 kg uncontaminated soil (dilution ratio 1:9) to obtain a final concentration of fresh PHE of 300 mg kg^{-1}.

2.2. Bacterial strain

Achromobacter sp. LH-1 were isolated from soil sample obtained from the Daqing Oilfield in China and then stored in our laboratory. (substrate concentration, 100 mg L^{-1}; pH, 7; inoculum size, 5%, culture time, 7d; temperature, 28.1°C; degradation rate, 97.48%) [22].

2.3 Biochar preparation and characterization

Biochar was created in a programmable tube furnace (Jinan Jingrui Instrument Co., Ltd., China) through slow pyrolysis. Briefly, the straw was air-dried and ground to less than 2 mm and pyrolyzed at a heating rate of 5 °C min^{-1} under N_2 conditions for 4 h. Final temperatures of 300, 500, and 700 °C were used, and the produced biochars were allowed to cool to room temperature after pyrolysis. For simplicity, the biochars were denoted as BC 300, BC 500, and BC 700, where BC represents biochar and the numbers represent the final temperature. All biochars were milled to a homogenous fine powder using a ball mill to pass a 2-mm sieve and dried overnight at 105°C prior to being analyzed.

The biochar yield was calculated by the following equation:

$$\text{Biochar yield } (\%) = \frac{\text{Biochar we ight}}{\text{Raw materal weight}} \times 100\% \qquad \text{(ref. 1)}$$

Ash matter contents was calculated from the residual weight obtained after heating at 815 ± 1 °C for 2 h in a muffle furnace (National Standard of the People's Republic of China). The ash yield was calculated by the following equation:

$$\text{Ash yield } (\%) = \frac{\text{Ash weight}}{\text{Raw materal weight}} \times 100\% \qquad \text{(ref. 2)}$$

As for the pH of biochar sample, mixed dried sample to water ratio of 1:20 (w/v) and stirred for 60 min. The obtained supernatant after centrifugation was used to determine the pH with a pH meter (Mettler Toledo, ME403E). Contents of C, H, N, and S in the biochar were determined using an elemental analyzer (Vario EL/micro cube, Elementar, Germany). The oxygen content was calculated by subtracting C, N, H, S, and ash contents from the total char mass. The surface functional groups of biochars were characterized by Fourier transform infrared (FTIR) spectroscopy (Varian 640-IR, USA) in a wavelength range of 400–4000 cm^{-1} using KBr pellets. Sigma Plot 10.0 software was used for drawing figures. The microstructures of the synthesized composites were characterized by scanning electron microscopy (SEM, ZEISS SUPRA40) [23, 24]. All analyses were conducted in triplicate.

2.4 Immobilization of LH-1 cells on biochar

The composition of the Luria-Bertani (LB) was as follows: yeast extract 10 g L^{-1}, peptone 5 g L^{-1} and NaCl 10 g L^{-1} [25]. For the preparation of cell suspensions, one loop of isolate was picked up and inoculated into a liquid LB. After 18 h incubation on a rotary shaker at 27°C 150 rpm, the cells grew to the logarithmic growth phase and were then harvested. The cell culture was centrifuged at 8000 r min^{-1} for 5 min, rinsed 3 times, and resuspended; thereafter, the cell suspension was condensed (OD600 = 2.0 ± 0.1) and prepared for further inoculations.

To immobilize LH-1 cells on rice straw biochar, 5 g biochar (dry weight) was then soaked with fresh mineral salt medium (MSM) (1:20, w/v) in 150 mL flasks. Subsequently, the cells were sterilized at 121°C for 30 min [26]. After cooling, cell suspensions were introduced to the flasks, with each flask receiving 5 mL of condensed cell suspension. The flask contents were then incubated on a rotary shaker at 30°C and 80 rpm for 48 h. The mixtures were separated with a 75-μm sieve and rinsed with deionized water thrice to remove the planktonic cells. The obtained LH-1-composite should be collected and stored at 4°C if immediate inoculation into soil is not possible [27]. All operations were performed under strict aseptic conditions.

2.5 Soil remediation test

The experiment used the potting method for ryegrass cultivation [28], and 2 kg of soil was weighed for each pot. In this pot trial, six treatments with three replicates were carried out: addition of 1% biochar (BC), addition of 1% biochar and 300 mg/kg PHE (PBC), addition of 1% *Achromobacter* sp. LH-1 and 300 mg kg^{-1} PHE (PLH), addition of 1% bacterial inoculant (biochar + *Achromobacter* sp. LH-1) and 300 mg kg^{-1} PHE (PCLH), addition of 300 mg kg^{-1} PHE (SPHE), and untreated soil (CK).

The main applications were as follows. We weighed 2 kg each of non-recontaminated soil and PHE-contaminated soil, a mixture of soil with biochar and a mixture of soil with a bacterial inoculant into each pot, and we activated the soil microbes by incubating the soil for 10 days at a water content of approximately 50% WHC (water holding capacity). After ryegrass seeds vernalized at 4°C, the ryegrass seeds were sterilized in 30% H_2O_2 for 20 min, washed, and then balanced for 24 h. The sowing depth was 2–3 cm. After growing seeds in the pots, ryegrass was grown at a temperature of 30°C during the day and 22°C at night for 45 days. The water content was maintained at approximately 50% WHC, and fertilizer was not added during incubation. The position of the pots was randomly exchanged every 2 days. Independent triplicates were performed for the six conditions, for a total of 18 pots. Each pot had 40 ryegrass seedlings [29].

After 45 days, measured the seedling length and weight of ryegrass and retrieved the soil sample from each pot, and then removed roots from the soil sample. Each pot's soil sample was divided and stored differently as required. One subsample of the rhizosphere soil was collected for the determination of high-throughput sequencing and shotgun metagenomics. The remaining sample was sieved with a 2-mm sieve to remove biochar particles, after which some was freeze-dried to detect phenanthrene (PHE) concentrations and some was air-dried to analyze soil physicochemical properties.

2.6 Soil physicochemical property

For the pH of the soil sample, approximately 10 g of dried sample, sieved through 10 meshes, was mixed with 25 mL distilled water and stirred for 30 min. Finally, the obtained supernatant after centrifugation was used to determine the pH with a pH meter [30]. The water content of the soil was determined by subtraction. The quality was calculated by the subtracting the constant weight of soil dried at 105℃ in triplicate from the wet soil value. The soil organic matter was measured using the potassium dichromate capacity method (diluted heat method), the total nitrogen was measured using semi-micro-Kelvin method [31], the total phosphorus was measured using $HClO_4$-H_2SO_4 method [32], and the total potassium was determined by flame photometry with NaOH melting [30]. All analyses were conducted in triplicate.

2.7 Extraction and quantification of PHE

High-performance liquid chromatography (HPLC) was used to detect soil PHE quantification. The Philippine standards (98.7% purity) were purchased from Sigma-Aldrich (America). Briefly, frozen soil was sieved through a 100 mesh sieve, and then ultrasonic extraction with dichloromethane (1:12.5, w/v) (Tianjin Komeo Chemical Reagent Co., Ltd., chromatographic grade) was used for 10 min. The suspension was centrifuged at 4000 rpm for 5 min, and the supernatant was decanted. This procedure was performed thrice. The elute was concentrated via the rotary evaporation method, dissolved in 5 mL of methanol (Zidi ma Technology Co., Ltd., chromatographic grade), and filtered through a 0.22-μm organic filter before column chromatography [33, 34].

The HPLC conditions were as follows: The mobile phase was 70% acetonitrile (Zidi ma technology co., Ltd., chromatographic grade) and 30% ultrapure water at flow rate of 1.5 mL L^{-1}. The analysis time was 10 min and the injection volume was 10μL. The experiment was repeated three times.

2.8 DNA extraction, amplification and sequencing

The soil samples from CK, BC, SPHE, PBC, PLH, and PCLH in triplicate were sent to Shanghai Sangon Biological Co., Ltd. for high-throughput and metagenome sequencing. Genomic DNA was extracted from the microbial community samples with the E.Z.N.A™ Mag-Bind Soil DNA Kit (Omega Bio-Tek, GA, USA) according to kit and instrument protocols. DNA was stored at -20 °C until further processing. Two PCR amplifications were performed. The first PCR amplification of the V3-V4 region of the 16S rRNA genes was PCR amplified with 341F (5'-CCCTACACGACGCTCTTCCGATCTG-3') and 805R (5'-GACTGGAGTTCCTTGGCACCCGAGAATTCCA-3') primers containing barcodes at the 5' end of the front primer. PCR was performed in 30 μl reactions containing 1 μl of Bar-PCR primer F (10 μM), 15 μl of 2 × Taq master Mix, 1 μl of Primer R (10 μM) and up to 10–20 ng of genomic DNA. The PCR process was as follows: initial denaturation at 94℃ for 3 min; 5 cycles of 94℃ for 30 s, 45℃ for 20 s, and 65℃ for 30 s; 20 cycles of 94℃ for 20 s, 55℃ for 20 s, and 72℃ for 30 s; and final extension at 72℃ for 5 min. A second round of amplification was conducted after the PCR. The second PCR amplification introduced Illumina bridge PCR compatible primers. PCR was performed in 30 μl reactions containing 1 μl of primer F (10 μM); 15 μl of 2 × Taq master Mix; 1 μl of Primer R (10 μM) and up to 20 ng of PCR products (from first PCR amplification). The PCR process was as follows: initial denaturation at 95 ℃ for 3 min; 5 cycles of 94 ℃ for 30 s, 55 ℃ for 20 s, and 72 ℃ for 30 s and final extension at 72 ℃ for 5 min. PCR products for each sample were purified using the E.Z.N.A. Gel Extraction Kit (Omega Bio-Tek, Inc., GA, USA) and then quantified using the Qubit3.0 DNA Test Kit (Life, CA, USA). Equal amounts of PCR products were pooled to produce equivalent sequencing depths from all samples. After purification with the Agencourt AMPure XP KIT, the pooled PCR products were used to construct a DNA library using the NEB E7370L DNA Library preparation kit according to instructions from Illumina. Finally, the single composite barcoded PCR product was sequenced on an Illumina MiSeq™ machine using the PE250 protocol.

2.9 Analysis of microbial community composition and diversity in soil

The soil samples from CK, BC, SPHE, PBC, PLH, and PCLH in triplicate were sent to Shanghai Sangon Biological Co., Ltd., for high-throughput sequencing to determine the relationship among the bacterial communities in the soil samples [35]. Sequenced reads were subjected to the Cutadapt program (version 0.1.123) with -O 5 -m 50. Subsequent quality cuts of reads used the Prinseq program with the -lc_method dust -lc_threshold 40 -min_len 200. The trimmed paired reads were combined by the PEAR program (version 0.9.5) with a p-value of 0.01. More than 60,000 raw sequences for each sample were obtained for data analysis on average. Usearch was used to remove non-amplified region sequences, the sequences were corrected, and uchime was used to identify chimeras. The sequence of the removed chimera was blastn-aligned with the representative sequence of the database to remove alignment results below the threshold. Operational taxonomic units (OTUs) were picked (clustered at 97% similarity), and by plotting the relationship between the change in the number of OTUs and the similarity value of the cluster, the best similarity value was selected for OTU analysis and taxonomic analysis. The alpha diversity of the samples was estimated by Chao1 richness estimators and the inverse Simpson diversity index. Each sequence was species classified by the naïve Bayesian assignment algorithm using the RDP classifier (RDP classification threshold > 0.8).

2.10 Metagenome sequencing, processing and data analysis

SPHE, PBC and PCLH samples were subjected to metagenome sequencing by Roche 454 pyrosequencing approaches. The total genomic DNA of each soil sample extracted using the E.Z.N.A™ Mag-Bind Soil DNA Kit (QIAGEN, 51504) of OMEGA. Library construction and sequencing were carried out by Shanghai Shengon Biological Co., Ltd., using standard shotgun protocols to obtain 40,781,536 – 52,804,630 raw reads per sample, with an average length of 150 bp for each sample. FastQC and Trimmomatic programs were used to quality control the sequences with a 0.01 maximum error rate, leading to 133,482,380 high-quality sequences. Prodigal was used for gene prediction, as it can predict high-quality gene fragments by short reads and surmounts homopolymer errors. BLAST searching protein sequences against the NCBI nr database was used to assign functional and taxonomic assignments of the predicted genes. Allocating KEGG orthologies to genes in the metagenome was conducted through the Ghost-KOALA annotation server and by rebuilding metabolic

pathways. Statistical differences in the abundance of gene families involved in the C, N, P and S element cycles were measured by response ratio analysis. We mapped and explored alterations of genes and then speculated on the alterations of elemental circulation and the ecological environment caused by the addition of biochar and PHE-degrading bacterial inoculant during the repair process of PHE-contaminated soil.

3 Results And Discussion

3.1 Yield and ash of biochars

The yields, elemental compositions and ash contents, atomic ratios and pH of the biochar derived from straw at the 300℃, 500℃ and 700℃ temperatures are listed in Fig. 1 and Table 1. Biochar production is inversely proportional to pyrolysis temperature because of the large amount of cellulose and hemicellulose contained in rice straw, which ranged from 26.6 to 49.6 wt%. The ash content of BC300 (biochar prepared at 300℃) was 13.83%, which was lower than that of BC500 and BC700. This difference may be caused by the incomplete volatilization of cellulose and hemicellulose at lower pyrolysis temperatures. The ash contents of BC500 (biochar prepared at 500℃) and BC700 (biochar prepared at 700℃) were 17.25% and 29.95%, respectively, indicating that as the pyrolysis temperature increased, the proportion of non-volatile ash increased. The amount of ash produced by pyrolysis was close to one-third of the total production of biochar at the pyrolysis temperature of 700℃. BC300 had the highest yield and the lowest ash content. BC700 had a relatively lower yield and an extremely high ash content, which also required higher energy consumption in the preparation process. Therefore, BC700 should be avoided in actual production.

3.2 Elemental analysis and pH of biochars

Table 1
pH and elemental analysis of biochars (BC300, BC500 and BC700). BC refers to the biochar obtained from rice straws; 300, 500 and 700 are the heating treatment temperatures.

Samples	pH	elements(%)						atomic ratio (%)			
		C	H	N	O	P	S	(N+O)/C	H/C	(C+H)/O	O/C
BC300	7.49	54.91	3.04	1.29	21.61	0.73	0.92	0.417	0.053	2.681	0.393
BC500	10.14	57	1.72	1.08	15.01	0.76	0.74	0.282	0.03	3.912	0.263
BC700	10.31	63.35	0.95	1.12	6.93	0.73	0.62	0.127	0.014	9.278	0.109

The pH of biochar is directly proportional to the pyrolysis temperature, and the pH values of BC300, BC500 and BC700 were 7.49, 10.14 and 10.31, respectively. The C content in biochar (≥ 54.91) was the highest compared with H, N, O, P and S. The C contents of BC300, BC500 and BC700 were 54.91%, 57.00% and 63.35%, respectively, indicating that the C content of BC700 was significantly higher than that of the other two. The H contents of BC300, BC500, and BC700 were 3.04%, 1.72%, and 0.95%, respectively, and the O contents were 21.61%, 15.01%, and 6.93%, respectively, which means that the contents of H and O decreased as the temperature increased. O and H combined to form vapor that disappeared as the pyrolysis temperature increased, thereby reducing the element content. In contrast, C continued to accumulate through carbonization and increased in proportion. The atomic ratio can usually be used to reflect the physicochemical properties of biochar. The degree of aromatization of biochar also increased with increasing pyrolysis temperature. The H/C ratios of BC300, BC500, and BC700 were 0.053, 0.030, and 0.014, respectively, which were affected by the degree of carbonization being directly proportional to the pyrolysis temperature during the preparation of biochar. Moreover, large amounts of aromatic ring structures were produced, which gave them a high degree of aromatization. All three biochars had high reducibility and good stability, and BC700 had special reduction and stability characteristics. From the perspective of elemental analysis, the difference in polarity, reducibility and stability of biochars may be the main reason for their different properties and functions.

3.3 Fourier transform infrared spectroscopy (FTIR) analysis of biochars

Figure 2 shows the FTIR spectra of biochars. The vibration position appeared in the same band, but the intensities of the main significant peaks were different. In general, the degree of carbonized biochar increased with the loss of functional groups. The broad band at 3400 cm^{-1} was due to the O-H stretching vibration in the carboxyl and phenolic hydroxyl groups because the O-H structure contained in the cellulose, hemicellulose and lignin was not destroyed completely in the processes of pyrolysis and carbonization. As the pyrolysis temperature increased, the peak became less pronounced in biochar, indicating that the O-H structure was well preserved in BC300 and BC500, while that in BC700 was seriously damaged after pyrolysis carbonization. The band intensity between 3000 and 2800 cm^{-1} was related to aliphatic group stretching. The band strength of biochar was positively related to the pyrolysis temperature because of condensation and polymerization. This result was connected with the differences in the O/C and H/C of biochar (Table 2). The peak at about 1640 cm^{-1} may because of -OH and C = O vibrations. The peaks of BC300 and BC500 were similar, while the band intensity of 700BC became weaker, which proved that the temperature at 700°C have a strong decarboxylation reaction, while the reaction of BC500 was similar to BC300. The band at 1400 cm^{-1} was have connection with -COOH stretching, and the increased of intensity have connection with pyrolysis temperature increase. This was related with the peaks at 468.84 cm^{-1}, 486.03 cm^{-1} and 464.57 cm^{-1} associated to -CH stretching vibration. The broad band between 1000 cm-1 and 1300 cm-1 was related to alcohols (C-O) stretching, which was cellulose and hemicellulose characteristic. The broad band of biochar between 1000 cm^{-1} and 1300 cm^{-1} decreased with pyrolysis increases. The peaks at 464 cm^{-1} and 473 cm^{-1} were attributed to -CH stretching vibration. The peaks at 786 cm^{-1}, 801 cm^{-1} and 804 cm^{-1} were attributed to the presence of aromatic substances in the material. The band intensity of BC700 was significantly weaker than that of the BC300 and BC500, indicates excessive temperatures resulting in the breaking of functional group bonds and the reduction of functional groups. The difference in the strengths of the functional groups was one of the main reasons for the difference in biochar properties and functions.

3.4 Scanning electron microscope (SEM) analysis of biochars

The SEM images in Fig. 3, enlarged multiples 2 k (left) and 5 k (right), neatly display the dramatically different surface and pore structures of the three kinds of biochar. Compared with BC300, the surfaces of BC700 were more damaged (Fig. 3, left). The surfaces of biochar particles (BC500 and BC700) were relatively rough and porous, with massive substances (Fig. 3, right). The difference in porosity was uniformly distributed on the biochar surface, and this was the key reason for the difference in biochar adsorption performance. Therefore, BC500 and BC700 had better adsorption and an easier diffusion process in the adsorbate particles effect than did BC300, which improved the adsorption efficiency in the pores. Through the analyses of elemental, SEM and FTIR, it could be concluded that straw pyrolysis at 500°C formed biochar with the best application performance.

3.5 The degradation of phenanthrene

The experiment was carried out with 4 treatments: SPHE, PLH, PBC and PCLH; the amount of degraded PHE was measured after 45 days of incubation. The residual PHE in the soil was 45.7%, 24.3%, 14.6%, and 6.6%, respectively (Fig. 4). The decrease in PHE in SPHE may be because of the plants that were planted and some microorganisms of the original microbes in the soil degraded the PHE. The PHE in surface soils were easily volatized or degraded under long-term lighting. The PHE residue curve showed that the soil PHE concentration in the PBC and PCLH decreased rapidly with residual ratios of 50.8% and 47.9% at 15 days, respectively (Fig. 4), which indicates that biochar had a relatively fast adsorption of organic pollutants, implying that biochar could improve contaminated soil effectively in a short time. The SPHE degradation rate was faster in the middle of the experiment, which indicated that the ryegrass gradually matured with the absorption of more pollutants. Therefore, the role of plants in the process of treating contaminated soils was equally important. Similar results have been reported in that plants could also support the degradation of PHE by improving the microbial population, soil physiochemical properties and adsorption of pollutants in the rhizosphere.

PCLH and PBC had the more efficient degradation in PLH, PBC and PCLH (75.7%, 85.4% and 93.4%), implying that biochar can adsorb soil pollutants and reduce the amount of pollutants in the soil. Among the six treatments, PCLH was the most degradable treatment, which indicates that the PHE-degrading bacteria adsorbed on the bacterial inoculant could degrade the PHE adsorbed into biochar. The above results indicated that biochar and bacterial inoculant had obvious repairing effects on the PHE-contaminated soil; they could effectually reduce soil pollutant content and toxicity and improve the soil ecological environment. Meanwhile, because PCLH and PBC had a fast adsorption speed and a remarkable effect, they had suitable repair performance in terms of improving PHE-contaminated soil.

3.6 Effects of biochar and phenanthrene degrading bacterial inoculant on the physiochemical properties of phenanthrene-contaminated soil

The soil microorganisms, plant growth and reproduction changed with the changes in water content. The water contents of treatments CK, BC, PBC, PCLH, PLH, and SPHE were 6.20%, 6.03%, 6.30%, 8.03%, 8.23%, and 8.20%, respectively (Fig. 5a). The soil water contents of the treatments with biochar (first three groups) were increased by approximately 2% compared with the treatments without biochar (last three groups), indicating that biochar addition to soil might make it possible to change the soil porosity and agglomeration, which affects the soil water retention capacity. The soil pH was significantly different in the 6 treatments, with pH values of CK, BC, PBC, PCLH, PLH and SPHE of 7.44, 7.81, 7.80, 7.76, 7.42 and 7.48, respectively (Fig. 5b). The pH of BC was found to be significantly higher than that of CK, indicating that biochar increased the pH of the soil because biochar, an alkaline substance, can continuously supply alkalinity to the soil during its application. The use of bacterial inoculant in the process of PHE-contaminated soil treatment increased the pH of the soil as well, implying that these two methods could improve the acidity of the soil in the process of soil pollution remediation. The organic matter content of CK, BC, PBC, PCLH, PLH and SPHE was 32.4 g kg^{-1}, 46.68 g kg^{-1}, 47.29 g kg^{-1}, 38.54 g kg^{-1}, 28.02 g kg^{-1} and 34.24 g kg^{-1}, respectively (Fig. 5c). Biochar addition in nonpolluted soil increased the organic matter content by 44.07% because the incomplete pyrolysis of biochar results in a large amount of carbon-containing compounds that slowly flow to the soil and increase the soil organic matter content. The biochar and bacterial inoculant improved the soil organic matter by 38.11% and 12.56%, respectively, implying that the biochar and bacterial inoculant were soil remediation agents and good soil amendments.

The total N, P and K contents in the soil at 45 days are shown in Fig. 5. The total N contents of treatment CK, BC, PBC, PCLH, PLH, and SPHE were 0.89 g/kg, 1.02 g/kg, 1.05 g/kg, 1.01 g/kg, 0.84 g/kg, and 1.01 g/kg, respectively (Fig. 5d). The increase in soil total N by biochar addition indicated that biochar was rich in N and carried N into the soil. The total N content in PLH and PCLH was lower than that in PBC, which may be because a large amount of exogenous bacteria was brought in by PLH and PCLH. These exogenous bacteria promoted N consumption in the soil, resulting in a lower total N content than that in PBC. The trend of total P was similar to that of N in soil. The total P of treatment CK, BC, PBC, PCLH, PLH and SPHE were 0.83 g/kg, 0.93 g/kg, 0.91 g/kg, 0.89 g/kg, 0.79 g/kg, and 0.84 g/kg, respectively (Fig. 5e). Biochar addition increased the soil total P by 12.04%. The total P of PBC was increased by 5.95% compared with SPHE, and PLH was reduced by 7.976% compared with SPHE. The change in P in different groups was not obvious. The total K of treatment CK, BC, PBC, PCLH, PLH, SPHE were 17.2 g/kg, 20.1 g/kg, 19.7 g/kg, 18.7 g/kg, 16.8 g/kg, and 18.3 g/kg, respectively (Fig. 5f). The increase in the content of total K compared to CK was 16.86% for BC and 2.1% for PCLH, while it decreased by 8.19% for PLH. The content of total K of PLH was lower than that of PLH, and they were both lower than that of PBC. The decrease in the total K of PLH was caused by the addition of exogenous microorganisms. These results showed that biochar and bacterial inoculant addition in the PHE-contaminated soil degraded the total NPK and organic matter but significantly increased the soil water content and soil pH. These ingredients were the essential materials for the growth of plants and microorganisms, implying that biochar and bacterial inoculant addition could effectively reduce pollution and increase soil nutrients and fertility levels.

3.6 Effects of biochar and phenanthrene degrading bacterial inoculant on the ryegrass

Ryegrass, because of its well-developed root system, can respond to soil changed in a timely manner, so it was used as an indicator plant in this experiment. After 45 days of experiment, the average seedling length of the SPHE was 27.3% less than that of the CK, indicating that PHE pollution inhibited the growth

of ryegrass in soil (Fig. 5g). The average length of ryegrass in the BC was 7.94% increased than CK, indicating that biochar addition promoted the growth of ryegrass, which may be because biochar releasing its own nutrients into the soil, thereby improving soil properties and fixing nutrients. The average seedling length of PBC, PLH and PCLH were 18.9%, 15.8% and 42.7% higher than that of SPHE, respectively. It implied that the repair method of the bacterial inoculant had the greatest effect on the growth of ryegrass, which could restore the length of ryegrass to the level of non-polluted soil.

After 45 days of experiment, the average weight of ryegrass in the BC was 11.7% increased than CK, indicating that biochar addition promoted the growth of ryegrass (Fig. 5h). The average seedling weight of ryegrass in the SPHE group was 31.2% lower than that in the CK group, indicating that PHE pollution inhibited the growth of ryegrass. The seedling weight of the PBC, PLH and PCLH groups was higher than that of the SPHE group, which was because all three treatments reduced the concentration of PHE in the soil, thereby reducing the toxicity of PHE in the soil, and thus reducing its inhibition of the growth of ryegrass. In summary, the application of biochar and bacterial inoculant can promote the growth of ryegrass and restore the weight and length of ryegrass to normal levels. It indicated that biochar and bacterial inoculant were suitable as soil amendments for remediation of PHE-contaminated soil.

3.7 Bacterial diversity and community structure in soil

Table 2
Number of sequences analyzed, OTUs, estimated community richness estimators (Chao and ACE) and community diversity indices (Shannon and Simpson) of the 16S rRNA libraries of the samples

Sample ID	Clean num	Mean len	OUT num	Shannon index	Chao1 index	Coverage
CK	43750	420.59	4035	6.79	5548.16	0.96
BC	43201	421.28	3985	6.58	5614.95	0.96
SPHE	51615	419.02	4035	6.54	5401.42	0.97
PBC	49303	419.48	3981	6.66	5468.70	0.97
PLH	53580	419.43	3407	6.06	5015.33	0.97
PCLH	45560	417.48	3380	6.36	4991.04	0.97

To understand the community changes and explore the relationships between the community changes and PHE degradation, 16S rRNA gene sequencing data were collected and analyzed. Based on the next-generation sequencing (NGS) results, 287,009 valid reads across the 6 samples were obtained after quality control measures. The coverage index (Table 2) ranged from 83–92%, which indicated that these results truly reflected the majority of bacterial community information in the sample. The Shannon index and Chao1 index of CK were higher than those of SPHE because PHE contamination inhibited the growth of a large number of microorganisms. The Shannon index declined after biochar addition in soil, but the Chao1 index increased, which meant that the species diversity was lower and the species richness was higher. This result may be because biochar addition increased the total abundance of soil species but destroyed the uniformity of the species. However, biochar addition to contaminated soil increased both the Chao1 and the fragrance index, implying that biochar addition reduced the soil PHE concentration and had a positive effect on soil microbes, which was similar to the results of previous research. PLH and PCLH had the lowest species richness, which indicated that the added PHE-degrading bacteria could use PHE as a carbon source to grow into a dominant flora and destroy the microbial balance in the original soil, resulting in a decrease in microbial abundance in the soil. However, the degradation of PHE in PLH and PCLH was higher than that in others, indicating that the addition of degrading bacteria and bacterial inoculant had positive effects in terms of repairing contaminated soil.

The abundance of bacteria at the phylum level and genus level was examined. Phylogenetic assignments from 31 phyla and 48 genera of 6 soil samples were identified. The most abundant phyla among the 6 samples were Proteobacteria, Acidobacteria, and Verrucomicrobia, whose richness exceeded 50% of all soil phyla, indicating that these 3 bacteria were the dominant phyla in the soil (Fig. 6a). The abundance of soil microbes changed greatly during the restoration process. The abundance of *Achromobacter* sp. in the PLH and PCLH groups was significantly increased compared with that in PHE (SPHE: 0.03%, PLH: 1.99%, PCLH: 2.43%), implying that the addition of LH-1 can be stably present in the soil (Fig. 6b). The abundance of *Achromobacter* sp. in PCLH was higher than that in PLH, implying that biochar could effectively immobilize the addition of LH-1 in soil. The abundance of *Sphingobacterium* sp. (PBC:9.35%, PLH:14.1%, PCLH:10.67%), *Subdivision 3 genera Incertae sedis* sp. (PBC:3.36%, PLH:3.05%, PCLH:4.11%), *Ohtaekwangia* sp. (PBC:2.63%, PLH:1.57%, PCLH:2.46%) and *Lysobacter* sp. (PBC:0.96, PLH:3.69%, PCLH:1.84%), were greater in PBC, PLH and PCLH than in SPHE and recovered to CK levels during processing (Fig. 6b). This result may be because these three treatments reduced the PHE in soil, leading to changes in the soil microenvironment and resulting in the slow recovery of some bacteria.

3.8 Bacterial diversity and community structure in soil

The links between PHE degradation and soil bacteria were analyzed for phylogenetic classification using principal coordinate analysis (PCoA) (Fig. 7). Each operational taxonomic unit (OTU) number is represented in the PCoA, and the correspondence of these OTUs with their taxonomic classification (obtained for a 97% similarity threshold) is presented in Table 3. We observed that in terms of PAH degradation, the abundance of 34 OTUs (out of 50) correlated well together, indicating that PHE degradation in soil may be highly correlated with Proteobacteria, Gemmatimonadetes, Bacteroidetes, and Actinobacteria, and particularly with the Micrococcaceae, Sphingomonadaceae, Comamonadaceae, Alcaligenaceae, Xanthomonadaceae, Gemmatimonadaceae and Chitinophagaceae families. The abundance of these bacteria in PCLH and PBC was high, and the degradation ability of both treatments was very high, indicating that PAH degradation was related to the abundance of specific bacteria that could metabolize them and to the proportion of these bacteria.

Therefore, in the following content, we specifically analyze the contribution of these microorganisms in the PHE metabolic pathway and analyze the differences between PBC and PCLH in the PHE metabolic pathway.

Table 3
Taxonomic correspondences of the abundance of 50 first OTUs in terms of abundance in the six studied soils at a similarity threshold of 97% with percentages of similarity.

	phylum	class	order	family	genus
Otu2545	Acidobacteria	Acidobacteria_Gp4	NA	NA	Gp4
Otu17478	Proteobacteria	Alphaproteobacteria	Sphingomonadales	Sphingomonadaceae	Sphingomonas
Otu12278	Proteobacteria	Alphaproteobacteria	Sphingomonadales	Sphingomonadaceae	Sphingomonas
Otu18554	Proteobacteria	Alphaproteobacteria	Sphingomonadales	Erythrobacteraceae	Porphyrobacter
Otu16369	Actinobacteria	Actinobacteria	Actinomycetales	Micrococcaceae	Arthrobacter
Otu18534	Proteobacteria	Alphaproteobacteria	Sphingomonadales	Sphingomonadaceae	unclassified
Otu187	Proteobacteria	Betaproteobacteria	Burkholderiales	Comamonadaceae	Ramlibacter
Otu18544	Proteobacteria	Alphaproteobacteria	Sphingomonadales	Sphingomonadaceae	Sphingomonas
Otu17944	Proteobacteria	Alphaproteobacteria	Sphingomonadales	Erythrobacteraceae	Altererythrobacter
Otu18540	Proteobacteria	Alphaproteobacteria	Sphingomonadales	Sphingomonadaceae	Sphingobium
Otu18537	Proteobacteria	Alphaproteobacteria	Sphingomonadales	Sphingomonadaceae	Novosphingobium
Otu17953	unclassified	unclassified	unclassified	unclassified	unclassified
Otu10027	Bacteroidetes	Cytophagia	Cytophagales	NA	Ohtaekwangia
Otu368	Proteobacteria	Betaproteobacteria	Burkholderiales	Alcaligenaceae	Achromobacter
Otu17947	unclassified	unclassified	unclassified	unclassified	unclassified
Otu370	Proteobacteria	Gammaproteobacteria	Xanthomonadales	Xanthomonadaceae	unclassified
Otu17480	Acidobacteria	Acidobacteria_Gp4	NA	NA	Blastocatella
Otu15723	Actinobacteria	Actinobacteria	unclassified	unclassified	unclassified
Otu18535	Proteobacteria	Alphaproteobacteria	Sphingomonadales	Sphingomonadaceae	Sphingomonas
Otu17948	Candidatus Saccharibacteria	NA	NA	NA	Saccharibacteria_genera_incertae_sedis
Otu18536	Acidobacteria	Acidobacteria_Gp4	NA	NA	Aridibacter
Otu1033	Actinobacteria	Actinobacteria	Gaiellales	Gaiellaceae	Gaiella
Otu372	Proteobacteria	Betaproteobacteria	Burkholderiales	Oxalobacteraceae	Massilia
Otu18539	Proteobacteria	Alphaproteobacteria	Sphingomonadales	Sphingomonadaceae	Sphingomonas
Otu10872	Gemmatimonadetes	Gemmatimonadetes	Gemmatimonadales	Gemmatimonadaceae	Gemmatimonas
Otu18541	Proteobacteria	Alphaproteobacteria	Sphingomonadales	Erythrobacteraceae	Porphyrobacter
Otu8880	Bacteroidetes	Sphingobacteriia	Sphingobacteriales	Chitinophagaceae	Terrimonas
Otu1102	Acidobacteria	Acidobacteria_Gp4	NA	NA	Gp4
Otu18538	Acidobacteria	Acidobacteria_Gp1	NA	NA	Gp1
Otu369	Verrucomicrobia	Verrucomicrobiae	Verrucomicrobiales	Verrucomicrobiaceae	Luteolibacter
Otu8881	Bacteroidetes	Cytophagia	Cytophagales	Cytophagaceae	Adhaeribacter
Otu2546	Verrucomicrobia	Spartobacteria	NA	NA	Spartobacteria_genera_incertae_sedis
Otu1034	Proteobacteria	Gammaproteobacteria	Xanthomonadales	Xanthomonadaceae	Lysobacter
Otu2636	Acidobacteria	Acidobacteria_Gp4	NA	NA	Gp4
Otu238	Acidobacteria	Acidobacteria_Gp7	NA	NA	Gp7
Otu375	Proteobacteria	Gammaproteobacteria	Xanthomonadales	Xanthomonadaceae	Lysobacter
Otu17991	Candidatus Saccharibacteria	NA	NA	NA	Saccharibacteria_genera_incertae_sedis
Otu7541	Bacteroidetes	Sphingobacteriia	Sphingobacteriales	Chitinophagaceae	Flavisolibacter
Otu7540	Bacteroidetes	Sphingobacteriia	Sphingobacteriales	Sphingobacteriaceae	Pedobacter

	phylum	class	order	family	genus
Otu8887	Bacteroidetes	Sphingobacteriia	Sphingobacteriales	Chitinophagaceae	Flavisolibacter
Otu1035	Acidobacteria	Acidobacteria_Gp7	NA	NA	Gp7
Otu19471	Proteobacteria	Alphaproteobacteria	Caulobacterales	Caulobacteraceae	Brevundimonas
Otu10854	Gemmatimonadetes	Gemmatimonadetes	Gemmatimonadales	Gemmatimonadaceae	Gemmatimonas
Otu385	Proteobacteria	Betaproteobacteria	Burkholderiales	Comamonadaceae	unclassified
Otu1036	Proteobacteria	Betaproteobacteria	Burkholderiales	Comamonadaceae	Hydrogenophaga
Otu4358	Verrucomicrobia	Spartobacteria	NA	NA	Spartobacteria_genera_incertae_sedis
Otu371	Proteobacteria	Gammaproteobacteria	Xanthomonadales	Xanthomonadaceae	Lysobacter
Otu4	Gemmatimonadetes	Gemmatimonadetes	Gemmatimonadales	Gemmatimonadaceae	Gemmatimonas
Otu17479	Candidatus Saccharibacteria	NA	NA	NA	Saccharibacteria_genera_incertae_sedis
Otu374	Proteobacteria	Gammaproteobacteria	Pseudomonadales	Pseudomonadaceae	Pseudomonas

3.9 Reconstruction of the phenanthrene metabolic pathway and contribution of microorganisms to metabolic steps

To determine which community members were involved in genes encoding PHE degradation-related enzymes, combining the results of the NCBI NR annotation pipeline and the GhostKOALA annotation pipeline, we mapped the PHE metabolic pathway. The first step of PHE degradation is catalysis by dioxygenase, where oxygen reacts with two adjacent carbon atoms (C-4 and C-5 positions) of the PHE, resulting in cis-3,4-dihydroxy-3,4dihydrophenanthrene formation. PAH dioxygenase large (K11943) and small (K11944) subunits participated in initial PHE oxidation. Cis-3,4-dihydroxy-3,4-dihydrophenanthrene is then metabolized by cis-3,4-dihydrophenanthrene-3,4-diol dehydrogenase (K18257) to form 3,4-dihydroxyphenanthrene, which is further metabolized to produce 1-hydroxy-2-naphthoic acid. Hydroxy-2-naphthoate is further metabolized through both the O-phthalate pathway and naphthalene pathway, leading to protocatechuate and salicylate, respectively. No salicylaldehyde dehydrogenase (K00152) was found in soil samples to degrade salicylaldehyde through the naphthalene pathway. However, benzaldehyde dehydrogenase (NAD) (K00141) was found in the soil, and its function is similar to that of K00152, allowing the degradation of salicylaldehyde to continue. Salicylaldehyde is dehydrogenated to form salicylate and then hydroxylated to produce catechol. Catechol was further degraded in three ways. Firstly, catechol could be metabolized through the catechol meta- and ortho-cleavage pathways, leading to intermediates of the tricarboxylic (TCA) cycle. Secondly, it could be converted to protocatechuate for further degradation. Thirdly, protocatechuate could be further metabolized through protocatechuate meta- and ortho-cleavage until finally entering the TCA cycle.

The genes encoding PHE degradation-related enzymes are mainly produced by Mycobacteriaceae and Commonarceaceae and have a good correlation with the degradation of PAHs in PCoA. In this consortium, *Mycobacterium rhodesiae* in the Mycobacteriaceae family was the main taxon that performed the early steps of PHE degradation, resulting in 1-hydroxy-2-naphthaldehyde (Fig. 8). Biochar induction significantly increased the abundance of *mycobacterium rhodesiae* (Fig. 9), suggesting that biochar induction could promote degradation and lead to a decrease in soil PHE content (Fig. 4). The exogenous microorganism LH-1 applied to PCLH was *Achromobacter* sp. Previous research found that LH-1 can degrade PHE through the salicylate pathway [36]. This is the same degradation pathway found in soil containing *Achromobacter* sp. It was found that the abundance of most species containing genes that convert naphthalene-1,2-diol to catechol in PBC and PCLH was greater than that in CK, and the increase in PCLH was greater than the increase in PBC. This result may be because the increase in *Achromobacter* sp. in the soil caused a large amount of PHE to be degraded by the catechol ortho-cleaving pathway, leading to an increase in the abundance of most species participating in this pathway. In addition, biochar addition increased the abundance of most species in the protocatechuic meta-cleavage pathway; in contrast, the addition of bacterial inoculant reduced the abundance of most species in the protocatechuic ortho-cleavage pathway.

The reconstructed catabolic pathway (Fig. 8) shows that soil PHE mineralizes in several pathways, as genes distributed to the catechol ortho- and meta-cleavage pathways and the protocatechuate ortho- and meta-cleavage pathways were detected. The addition of biochar and bacterial inoculant may reduce substrate competition between different degrading populations, thereby promoting the growth of soil PHE-degrading microorganisms, which can produce key enzymes in PHE degradation (Fig. 6), leading to PBC and PCLH. The residual amount of PHE was lower than that of PLH (Fig. 4). Our previous research showed that LH-1 could degrade PHE in the salicylate pathway and produce abundant intermediate metabolites in the degradation process [36], which increased the microbial activity that could utilize and degrade these intermediate metabolites. This process may be the reason why the abundance of most microorganisms in the catechol ortho-cleavage pathway in PCLH is higher than that in SPHE. This result is consistent with the Black Queen theory [37], in which one microorganism produces byproducts that will enhance the adaptability of other microorganisms capable of using these products [38].

In summary, biochar promoted microbial interactions to achieve PHE mineralization for metabolic steps by combining different symbiotic microorganisms. In most steps of PHE degradation, biochar increased the abundance of microorganisms that produced key enzymes. In contrast, the addition of bacterial inoculant mainly increased the abundance of microorganisms that produced key enzymes in the catechol ortho-cleavage pathway, indicating that PHE in PCLH is mainly carried out through the catechol ortho-cleavage pathway, which means that biochar in PCLH may play an auxiliary role and degradation is mainly processed by *Alcaligenaceae* sp. Regardless of the degradation effect or degradation pathway, the best treatment method is PCLH. However, the

addition of bacterial inoculant has affected the diversity of soil microorganisms to some extent; thus, a comprehensive analysis is needed in future applications.

3.10 Effects of biochar and bacterial inoculant additions on soil C cycling

The genes encoding C cycle-related enzymes were mainly contributed by Actinobacteria, Firmicutes and Proteobacteria (Fig. 10). Carbon metabolism is mainly divided into carbon anabolism and carbon catabolism, and microorganisms participate in carbon metabolism by participating in these two processes. The Calvin cycle is the most important way to fix CO_2 in microorganisms involved in C assimilation. The key enzyme of the Calvin cycle is RuBisCO. Biochar treatment reduced the abundance of the soil RuBisCO gene by 15.8% (Fig. 11a), indicating that biochar treatment had an inhibitory effect on soil C fixation. Biochar contained plentiful undecomposed and amorphous C that could be directly utilized or decomposed by microorganisms. This process causes the autotrophic microorganisms to lose their growth advantage, ultimately reducing C fixation [39]. Because biochar contains plentiful C sources, its application made the increment of soil C larger than the amount of C that was fixed. Bacterial inoculant addition increased the abundance of the RuBisCO gene in the soil by 74.02%, which may be because *Achromobacter* sp. in the bacterial inoculant was found to fix C through the metagenome (Fig. 10); thus, bacterial inoculant addition increased the abundance of the RuBisCO gene in the soil.

Another type of microorganism that participates in C metabolism is involved in organic C degradation, which is numerous and abundant. These microorganisms degrade organic carbon such as starch, cellulose, hemicellulose, fructose, chitin, and lignin. Starch is a relatively easy to degrade organic carbon compound. Biochar and bacterial inoculant had little effect on the abundances of the glucoamylase and alpha-amylase gene families; however, the abundance of the pullulanase gene family was obviously improved, indicating that biochar and bacterial inoculant had a promoting effect on soil starch metabolism (Fig. 11a). The abundances of soil gene families related to pectin- and hemicellulose-degrading enzymes were researched. Except for the pectin esterase and xylose isomerase gene families, biochar and bacterial inoculant addition obviously promoted the abundance of the gene family related to pectin- and hemicellulose-degrading enzymes (Fig. 11a). The above results indicated that biochar and bacterial inoculant promoted the metabolic process of soil, easily degrading C in the soil C cycle. Biochar and bacterial inoculant carry a large amount of soluble carbon compounds into the soil, providing nutrients for a large number of bacteria, which promotes the cycling process.

Cellulose is a typical agricultural waste that is relatively stable in soil, and its degradation is slow. Cellobiose phosphorylase, cellulase and endoglucanase are the main cellulose-degrading enzymes. Figure 11a shows that biochar and bacterial inoculant addition decreased the abundance of the cellobiose phosphorylase gene family but greatly increased the abundance of the cellulase and endoglucanase gene families. Overall, biochar and bacterial inoculant addition can promote soil cellulose metabolism. Chitin and lignin are the most difficult organic agricultural wastes [40]. Deacetylase and polyphenol oxidase are the main chitin- and lignin-degrading enzymes, respectively. Biochar addition partly decreased the abundance of the gene families that encoded these two enzymes, and bacterial inoculant reduced the abundance of polyphenol oxidase gene families. The decomposition of organic carbon in soil is carried out in an order from easy to difficult [34]. When biochar carries a large amount of soluble carbon into the soil, microorganisms preferentially degrade easily decomposable carbon compounds, which leads to biochar inhibiting soil chitin and lignin metabolism. Bacterial inoculant addition alleviated the inhibition of lignin degradation caused by biochar and promoted chitin degradation, which may be because *Achromobacter* sp. in the bacterial inoculant addition in PCLH has the ability to degrade chitin based on the metagenomic data, leading to the abundance of the gene families that encoded lignin-degrading enzymes to be slightly higher than that seen after the addition of biochar.

In summary, the C cycle in the three soil samples was mainly transformed by Actinobacteria, Firmicutes and Proteobacteria. Biochar and bacterial inoculant addition changed the gene families that encoded enzymes related to the C cycle and further changed the content of enzymes related to the soil C cycle. Biochar addition to PHE-contaminated soil promoted the degradation of relatively easy decomposable organic carbon compounds, thereby promoting the use of organic carbon compounds by soil plants, arthropods and microorganisms. However, biochar addition inhibited C fixation and lignin and chitin degradation, which are degradation-resistant agricultural wastes; thus, biochar addition may have adversely affected the C cycle in the soil to some extent. However, the inhibition of lignin and chitin degradation may also lead to soil C accumulation, which may compensate for the decline of C fixation to some extent. Bacterial inoculant addition in PHE-contaminated soil basically has similar effects as those of biochar on the C cycle. However, bacterial inoculant addition relieved the inhibition of lignin degradation and promoted chitin degradation and C fixation compared to biochar. This result may be because *Achromobacter* sp. in bacterial inoculant have the functions of chitin degradation and C fixation. This result provides a new possibility for improving polluted soil using biochar; specifically, biochar can be mixed with functional bacteria to balance the inhibitory effect of biochar on soil. Biochar and bacterial inoculant addition can promote the conversion of complex organic compounds into small-molecule compounds, promoting agricultural production and reducing chemical fertilizer application to some extent, which also protects the ecological environment. Currently, an increasing number of researchers are focusing on the disposal of agricultural waste, mainly cellulose-rich straw degradation. Biochar and bacterial inoculant addition could promote cellulose degradation, which presents more possibilities for agricultural production and ecological management.

3.11 Effects of biochar and bacterial inoculant addition on soil N cycling

In this study, nitrification, denitrification, dissimilatory nitrate reduction to ammonium and N_2 fixation were presented and analyzed. The gene families involved in the soil N cycle were mainly contributed by Proteobacteria, Actinobacteria, Bacteroidetes, Firmicutes and Thaumarchaeota (Fig. 10). Nitrification is the biological oxidation process that converts ammonia to nitrite and then to nitrate. *amo* encodes ammonia monooxygenase to control microbial biological nitrification. Biochar caused a reduction in *amo* abundance in soil by 83.9%, which may have been caused by the biochar addition changing the abundance of *amo* by affecting the abundance of *amo* ammonia-oxidizing microorganisms, which were influenced by experimental conditions and biochar properties such as fertilizer application and biochar feedstock [41]. The addition of the bacterial inoculant (Biochar + LH-1) increased *amo* abundance by 206.4% (Fig. 11b), which may be because *Achromobacter* sp. in bacterial inoculant was found to contribute *amo* in the metagenome.

In contrast, denitrification is a biological reductive process from NO_3^- to NO_2^-, NO, N_2O and ultimately N_2. The gene families including *narG*, *narJ* and *narH* control the NO_3^- reduction to NO_2^- (Fig. 10). Biochar and bacterial inoculant addition reduced the abundance of *narG* and *narH* (Fig. 11b), indicating that they have an inhibitory effect on this step in contaminated soil. Meanwhile, biochar contained plentiful nitrate; thus, it could be speculated that biochar and bacterial inoculant addition increased the soil nitrate concentration. The gene families including *nirS* and *nir*K control the NO_2^- reduction to NO (Fig. 10) and are considered target genes for measuring soil denitrification [42, 43]. Some studies found that soil N_2O emissions were positively correlated with *nirK/nirS* [41]. The impact of biochar and bacterial inoculant on the abundance of *nirS* was weak, while it significantly increased *nirK* abundance (Fig. 11b). This result may be because biochar improved soil aeration, thereby stimulating the growth and diversity of denitrifiers, leading to changes in gene family abundance [44–46]. The gene families including *norB* and *norC* control the denitrification of NO to N_2O (Fig. 10). Biochar or bacterial inoculant addition reduced *norB* abundance, while their application increased *norC* abundance (Fig. 11b) [47]. The gene families including *nosZ* control the N_2O reduction to N_2 (Fig. 10). Some studies have found that an increase in the abundance of nosZ leads to a reduction in N_2O emissions [48]. Biochar addition in PHE-contaminated soil reduced *nosZ* abundance, while bacterial inoculant addition increased *nosZ* abundance (Fig. 11b), which may be because that the effect of biochar addition on *nosZ* abundance may depend on the experimental conditions, such as planting, feedstock and pyrolysis temperature [41]. This result indicated that biochar addition to contaminated soil inhibited N_2O conversion. However, bacterial inoculant addition increased *nosZ* abundance. This difference may be because the *Achromobacter* sp. in bacterial inoculant was found to contribute to the *nosZ* gene family in the metagenome, which indicated that adding this kind of bacterial inoculant to contaminated soil may reduce N_2O emissions from soil.

Depending on the fate of the produced ammonium, nitrate reduction to ammonium in the environment is divided into dissimilatory and assimilatory nitrate reduction [49]. The assimilatory process is catalyzed by enzymes encoded by the *narB* (nitrate reductase), *nasA* (nitrate reductase) and *nirA* (nitrite reductase) gene families, while the dissimilatory process is catalyzed by enzymes encoded by *narG*, *narH*, and *narJ* (nitrate reductase) and by *nirB* and *nirD* (nitrite reductase) (Fig. 10). Biochar and bacterial inoculant addition greatly increased the abundance of *nasA* and *narB* and reduced the abundance of *narG*, *narJ* and *narH* to a lesser extent (Fig. 11b), indicating that their application may cause soil to carry out nitrate reduction mainly by assisting nitrate processes. The gene families of *nirA*, *nirB* and *nirD* usually coexist, and *nirA* expression requires *nirB* to provide a skeleton [50]. The abundance of *nirB* involved in assimilatory nitrate reduction did not change significantly, although biochar and bacterial inoculant addition inhibited *nirA* abundance (Fig. 11b). However, their addition increased the abundance of *nirD* to a large extent, indicating that their application promoted nitrate reduction, thereby reducing soil N loss. Biochar and bacterial inoculant addition increased the abundance of key enzymes in soil assimilation and dissimilation nitrate reduction, resulting in a large amount of NO_2^- being directly converted into ammonia in soil. On the one hand, there was reduced nitrogen loss from soil, and on the other hand, the N_2O production could be reduced, thereby protecting the ecological environment.

nif gene families encode nitrogenase to fix N_2 in soil and are considered an important source of ammonium. However, *nifG* was rarely detected in metagenomes, possibly due to random sampling issues in metagenomes. Nevertheless, *nifG* abundance changed significantly. Biochar and bacterial inoculant addition decreased the abundance of *nifG* in soil by 92% and 84%, respectively, indicating that biochar and bacterial inoculant addition may inhibit N_2 fixation, which may be because biochar improvement in wild plant species grown in soil would reduce soil nifG abundance [41].

In summary, the soil N cycle was mainly transformed by Proteobacteria, Actinobacteria, Bacteroidetes, Firmicutes and Thaumarchaeota. Biochar and bacterial inoculant application in soil changed the abundance of these microorganisms, thereby changing the abundance of the gene families that encoded enzymes involved in the N cycle. Biochar addition to contaminated soil may inhibit the conversion of N_2O to N_2, resulting in N_2O accumulation. However, its application promoted assimilatory and dissimilatory nitrate reduction. This process caused NO_3^- to be directly converted to ammonia in soil, thereby reducing soil N element loss. Moreover, the addition of biochar rich in NO_3^- further increased the soil N content and promoted the soil N cycle. This result may mean to reduce chemical fertilizer application in agriculture, thereby protecting the environment. In future practical applications, more attention should be paid to the increase in N_2O emissions and the inhibition of nitrification caused by the application of biochar. Bacterial inoculant addition to PHE-contaminated soil basically had similar effects as those of biochar on the N cycle. However, the addition of the bacterial inoculant addition increased the abundance of *nosZ* in denitrification and *amo* in nitrification compared to biochar, indicating that this kind of bacterial inoculant application can promote the conversion of N_2O to N_2 and nitrification, thereby reducing soil greenhouse gas N_2O emissions, promoting ammonia conversion, and slowing the greenhouse effect to promote soil N cycling. The result implies that the addition of bacterial inoculant, which use biochar as a carrier, to PHE-contaminated soil can not only make up for biochar deficiencies but also further promote soil nitrification and reduce soil N_2O emissions compared to biochar, thereby reducing greenhouse effects and protecting the environment.

3.12 Effects of biochar and bacterial inoculant addition on soil phosphorus and sulfur cycling

Soil microorganisms hydrolyze organic phosphorus into inorganic phosphorus through the secretion of extracellular enzymes (Fig. 10). Biochar and bacterial inoculant addition reduced the abundance of *ACP* (acid phosphatase) (Fig. 11c), which may be because biochar changed the pH buffering and nutrient input to affect the composition of soil microbial communities. Biochar addition reduced the abundance of *AKP* (alkaline phosphatase) (Fig. 11c), which may be because phosphatase is a constitutive rather than an induced enzyme and can be adsorbed onto clay and organic matter particles [51], implying that biochar addition to PHE-contaminated soil may inhibit organophosphorus hydrolysis to some extent. Bacterial inoculant addition increased the abundance of *AKP*, which may be because the *Achromobacter* sp. in our bacterial inoculant was found to contribute to the gene family encoding alkaline phosphatase in the metagenome (Fig. 11c), which alleviated the inhibitory effect of biochar on alkaline phosphatase. The contribution of alkaline phosphatase to soil organic phosphorus conversion may be higher than that of acid phosphatase [51], indicating that bacterial inoculant addition may

promote organic phosphorus conversion. The synthesis and decomposition of polyphosphates is an important process in the soil P cycle [52]. Biochar addition significantly reduced the abundance of *PPK* (polyphosphate kinase) but had less of an effect on the abundance of *PPX* (extraneous polyphosphatase), indicating that biochar greatly inhibited soil polyphosphates (Fig. 11c). bacterial inoculant addition had little effect on *PPK* and increased *PPX* abundance, indicating that the bacterial inoculant promoted polyphosphate degradation. Both treatments for repairing contaminated soils reduced the soil polyphosphate content. A large amount of polyphosphate in soil will cause water eutrophication as rainwater flows into rivers; thus, biochar and bacterial inoculant addition may reduce the environmental pollution of polyphosphate.

Soil S oxidation in this study was basically regulated by SOX (sulfur oxidase), which oxidizes sulfur to sulfite or sulfate in the S cycle [53]. Biochar and bacterial inoculant addition increased *SOX* abundance, indicating that biochar and bacterial inoculant promoted the oxidation process of soil sulfur metabolism. *dsrA*, *dsrB* (sulfate reductase) and *apr* (APS reductase) are recognized as the most critical enzymes in sulfur reduction, which is the conversion of sulfate or sulfite to H_2S. Biochar addition increased *dsrA* abundance but inhibited the abundance of *dsrB* and *apr*. bacterial inoculant addition increased *dsrB* abundance and reduced the abundance of *dsrA* and *apr*, indicating that biochar and bacterial inoculant addition inhibited S reduction and promoted S oxidation, implying that biochar and bacterial inoculant addition may reduce the conversion of sulfate or sulfite to H_2S, thereby reducing soil S loss. Their addition may promote oxidation to sulfite or sulfate, which will have beneficial effects on crops.

4 Conclusion

There is growing interest in using biochar and bacterial inoculant to improve PHE-contaminated soil. Using pot experiments, we investigated changes in soil physicochemical properties, the abundance of soil microbes involved in PHE degradation and the C, N, P and S cycling following biochar and bacterial inoculant addition to PHE-contaminated soil. It was found that the addition of biochar and bacterial inoculant increased the abundance of the majority of microorganisms involved in each part of the PHE degradation pathway, thereby promoting soil PHE degradation. Moreover, their addition enhanced soil C, N, P and S cycling, which promoted soil agricultural waste, such as straw, enhanced degradation, and reduced the loss of soil C and N and soil N_2O emissions. However, biochar addition inhibited C and N fixation and lignin and chitin degradation, which may create an unfavorable chemical environment for the evolution of microbial biomass [54]. bacterial inoculant addition partially mitigated the inhibitory effects in elements cycling caused by biochar addition, which indicated that microorganisms immobilized on biochar could be considered to reduce the adverse effects of biochar on soil. Thus, this research provides a new direction for pollutant metabolism and element cycling in contaminated soil. These results promote research on the use of biochar and bacterial inoculant to reduce soil pollutants and enhance C, N, P, and S bioavailability to crop plants in agroecosystems.

Abbreviations

PAHs: Polycyclic aromatic hydrocarbons. PHE: Phenanthrene. FTIR: Fourier transform infrared spectroscopy. SEM: Scanning electron microscopy. LB: Luria-Bertani. MSM: Salt medium. BC300: Biochar prepared at 300°C. BC500: Biochar prepared at 500°C. BC700: Biochar prepared at 700°C. BC: Soil with 1% biochar. PBC: Soil with 1% biochar and 300 mg/kg PHE. PLH: Soil with 1% *Achromobacter* sp. LH-1 and 300 mg kg^{-1} PHE. PCLH: Soil with 1% bacterial inoculant (biochar + *Achromobacter* sp. LH-1) and 300 mg kg^{-1} PHE. SPHE: Soil with 300 mg kg^{-1} PHE. CK: Untreated soil. WHC: Water holding capacity. HPLC: High-performance liquid chromatography. OTUs: Operational taxonomic units. NGS: Next-generation sequencing. PCoA: Principal coordinate analysis. TCA: Tricarboxylic cycle. K11943: PAH dioxygenase large subunits. K11944: PAH dioxygenase small subunits. K18257: Cis-3,4-dihydrophenanthrene-3,4-diol dehydrogenase. K00152: Salicylaldehyde dehydrogenase. K00141: Benzaldehyde dehydrogenase (NAD). *amo*: Ammonia monooxygenase. *narG*: Nitrite oxidoreductase, alpha subunit. *narJ*: Nitrate reductase molybdenum cofactor assembly chaperone NarJ. *narH*: Nitrite oxidoreductase, beta subunit. *nirK*: Nitrite reductase (NO-forming). *nirS*: Nitrite reductase (NO-forming). *norB*: Nitric oxide reductase subunit B. *norC*: Nitric oxide reductase subunit C. *nosZ*: Nitrous-oxide reductase. *narB*: Ferredoxin-nitrate reductase. *nasA*: Assimilatory nitrate reductase catalytic subunit. *nirA*: Ferredoxin-nitrite reductase. *narG*: Nitrite oxidoreductase, alpha subunit. *narH*: Nitrite oxidoreductase, beta subunit. *nirB*: Nitrite reductase (NADH) large subunit. *nirD*: Nitrite reductase (NADH) small subunit. *nifG*: Nitrogenase molybdenum-iron protein beta chain. *ACP*: Acid phosphatase. *AKP*: Alkaline phosphatase. *PPK*: Polyphosphate kinase. *PPX*: Extraneous polyphosphatase. SOX: Sulfur oxidase. *dsrA*: Dissimilatory sulfite reductase alpha subunit. *dsrB*: Dissimilatory sulfite reductase beta subunit. *apr*: Adenylylsulfate reductase.

Declarations

Ethics approval and consent to participate

Not applicable.

Consent for publication

Not applicable.

Availability of data and material

All data generated or analysed during this study are included in this published article.

Competing interests

The authors declare that they have no conflict of interest.

Funding

This research was supported by the Natural Science Foundation Excellent Youth Project of Heilongjiang Province (no. YQ2019E005), the Harbin Applied Technology Research and Development Funds (no. 2017RAYXJ020 and 2017RAYXJ019), the Postdoctoral Scientific Research Developmental Fund of Heilongjiang Province under grants no. LBH-Q16018, the Young Talent Fund of Northeast Agricultural University under grants no. 16QC12 and the Natural Science Foundation Project of Heilongjiang Province (no. C2016026).

Author contributions

NH, DPL and CYL designed the whole scheme of the study and conducted the experiments. QQW, XYL and XYZ wrote the manuscript and revised the manuscript.QQW, XYL, QYS and XXJ performed experiments, YG, LT, WZ and HLZ analyzed data. All authors read and approved the final manuscript.

Acknowledgements

Not applicable.

References

1. Crampon M, Bodilis J, Portet-Koltalo F. Linking initial soil bacterial diversity and polycyclic aromatic hydrocarbons (PAHs) degradation potential. J Hazard Mater. 2018;359:500–9.
2. Li S, Chang NY, Imhoff PT. Predicting water retention of biochar-amended soil from independent measurements of biochar and soil properties. Adv Water Resour. 2020;142:103638.
3. Zainudin MH, Mustapha NA, Maeda T, Ramli N, Sakai K, Hassan M. Biochar enhanced the nitrifying and denitrifying bacterial communities during the composting of poultry manure and rice straw. Waste Manage. 2020;106:240–9.
4. Prasai TP, Walsh KB, Midmore DJ, Jones BEH, Bhattarai SP. Manure from biochar, bentonite and zeolite feed supplemented poultry: Moisture retention and granulation properties. J Environ Manage. 2018;216:82–8.
5. Joseph S, Graber ER, Chia C, Munroe P, Donne S, Thomas T, Nielsen S, Marjo C, Rutlidge H, Pan GX, Li L, Taylor P, Rawal A, Hook J. Shifting paradigms: development of high-efficiency biochar fertilizers based on nanostructures and soluble components. Carbon Manag. 2013;4:323–43.
6. Quilliam RS, Glanville HC, Wade SC, Jones DL. Life in the 'charosphere' - does biochar in agricultural soil provide a significant habitat for microorganisms. Soil Biol Biochem. 2013;65:287–93.
7. Li X, Song Y, Wang F, Bian Y, Jiang X. Combined effects of maize straw biochar and oxalic acid on the dissipation of polycyclic aromatic hydrocarbons and microbial community structures in soil,A mechanistic study. J Hazard Mater. 2019;364:325–31.
8. Li X, Yao S, Bian Y, Jiang X, Song Y. The combination of biochar and plant roots improves soil bacterial adaptation to PAH stress: Insights from soil enzymes, microbiome, and metabolome. J Hazard Mater. 2020;17:123227.
9. Kong L, Gao Y, Zhou Q, Zhao X, Sun Z. Biochar accelerates PAHs biodegradation in petroleum-polluted soil by biostimulation strategy. J Hazard Mater. 2018;343:276–84.
10. Zhao JK, Li XM, Ai GM, Deng Y, Liu SJ, Jiang CY. Reconstruction of metabolic networks in a fluoranthene-degrading enrichments from polycyclic aromatic hydrocarbon polluted soil. J Hazard Mater. 2016;318:90–8.
11. Singha LP, Pandey P. Rhizobacterial community of Jatropha curcasassociated with pyrene biodegradation by consortium of PAH-degrading bacteria. Appl Soil Ecol. 2020;115:103685.
12. François T, Erwan C, Aurélie C. Stable isotope probing and metagenomics highlight the effect of plants on uncultured phenanthrene-degrading bacterial consortium in polluted soil. ISME J. 2019;13:1814–30.
13. Wu M, Guo X, Wu J, Chen K. Effect of compost amendment and bioaugmentation on PAH degradation and microbial community shifting in petroleum-contaminated soil. Chemosphere. 2020;256:126998.
14. Moulton OM, Altabet MA, Beman JM, Deegan LA, Lloret J, Lyons MK, Nelson JA, Pfister CA. Microbial associations with macrobiota in coastal ecosystems: patterns and implications for nitrogen cycling. Front Ecol Environ. 2016;14:200–8.
15. Ahmad M, YangQ, Zhang Y, Ling J, Sajjad W, Qi S, Zhou W, Zhang Y, Lin X, Zhang Y, Dong J. The distinct response of phenanthrene enriched bacterial consortia to different PAHs and their degradation potential: a mangrove sediment microcosm study. J Hazard Mater. 2019;380:120863.
16. Xu M, Gao P, Yang Z, Wu J, Yang G, Zhang X, Ma J, Peng H, Xiao Y. Biochar impacts on phosphorus cycling in rice ecosystem. Chemosphere. 2019;225:331–9.
17. Lehmann J, Rillig MC, Thies J, Masiello CA, Hockaday WC, Crowley D. Biochar effects on soil biota - a review. Soil Biol Biochem. 2011;43:1812–36.

18. Li S, Liang C, Shangguan Z. Effects of apple branch biochar on soil C mineralization and nutrient cycling under two levels of N. Sci Total Environ. 2017;607–608:109–19.
19. Fowler D, Coyle M, Skiba U, Sutton MA, Cape JN, Reis S, Sheppard LJ, Jenkins A, Grizzetti B, Galloway JN, Vitousek P, Leach A, Bouwman AF, Butterbach-Bahl K, Dentener F, Stevenson D, Amann M, Voss M. The global nitrogen cycle in the twenty-first century. Philos Trans R Soc B-Biol Sci. 2013;368:20130164.
20. Prommer J, Wanek W, Hofhansl F, Trojan D, Offre P, Urich T, Schleper C, Sassmann S, Kitzler B, Soja G, Hood-Nowotny RC. Biochar Decelerates Soil Organic Nitrogen Cycling but Stimulates Soil Nitrification in a Temperate Arable Field Trial. PLoS One. 2014;9:e86388.
21. Ibrahim MM, Tong C, Hu K, Zhou B, Xing S, Mao Y. Biochar-fertilizer interaction modifies N-sorption, enzyme activities and microbial functional abundance regulating nitrogen retention in rhizosphere soil. Sci Total Environ. 2020;739:140065.
22. Li C, Jia T, Fu M, Hou N, Cao H, Wang Q. Biodemulsifiers produced by Achromobacter sp. and their features in improving the biodegradation of phenanthrene. RSC Adv. 2017;7:4339–47.
23. Heikkinen J, Keskinen R, Soinne H, Hyväluoma J, Nikama J, Wikberg H, Källi A, Siipola V, Melkior T, Dupont C, Campargue M, Larsson SH, Hannula M, Rasa KK. Possibilities to improve soil aggregate stability using biochars derived from various biomasses through slow pyrolysis, hydrothermal carbonization, or torrefaction. Geoderma. 2019;344:40–9.
24. Yang X, Liu J, McGrouther K, Huang H, Lu K, Guo X, He LZ, Lin XM, Che L, Ye ZQ, Wang HL. Effect of biochar on the extractability of heavy metals (Cd, Cu, Pb, and Zn) and enzyme activity in soil. Environ Sci Pollut Res. 2016;23:974–84.
25. Li C, Chen X, Wen L, Cheng Y, An X, Li T, Zang H, Zhao X, Li D, Hou N. An enhancement strategy for the biodegradation of high-concentration aliphatic nitriles: Utilizing the glucose-mediated carbon catabolite repression mechanism. Environ Pollut. 2020;265:114302.
26. Zang H, Wang H, Miao L, Cheng Y, Zhang Y, Liu Y, Sun S, Wang Y, Li C. Carboxylesterase, a de-esterification enzyme, catalyzes the degradation of chlorimuron-ethyl in Rhodococcus erythropolis D310-1. J Hazard Mater. 2020;387:121684.
27. Lin CW, Wu CH, Huang WT, Tsai SL. Evaluation of different cellimmobilization strategies for simultaneous distillery wastewater treatment and electricity generation in microbial fuel cells. Fuel. 2015;144:1–8.
28. Kong L, Gao Y, Zhou Q, Zhao X, Sun Z. Biochar accelerates PAHs biodegradation in petroleum-polluted soil by biostimulation strategy. J Hazard Mater. 2018;343:276–84.
29. Zhou LS, Li H, Zhang Y, Han SQ, Xu H. Sphingomonas from petroleum-contaminated soils in Shenfu, China and their PAHs degradation abilities. Braz J Microbiol. 2016;47:271–8.
30. Xu HJ, Wang XH, Li H, Yao HY, Su JQ, Zhu YG. Biochar Impacts Soil Microbial Community Composition and Nitrogen Cycling in an Acidic Soil Planted with Rape. Environ Sci Technol. 2014;48(16):9397–9.
31. Quan G, Fan Q, Cui L, Zimmerman AR, Wang H, Zhu Z, Gao B, Wu L, Yan J. Simulated photocatalytic aging of biochar in soil ecosystem: Insight into organic carbon release, surface physicochemical properties and cadmium sorption. Environ Res. 2020;183:109241.
32. Prasad R. Determination of potentially available nitrogen in soils - a rapid procedure. Plant Soil. 1965;23:261–4.
33. Watanabe F, Olsen S. Test of an ascorbic acid method for determining phosphorus in water and NaHCO3 extracts from soil. Soil Sci Soc Am J. 1965;29:677–8.
34. Zhang Y, Wang F, Wei H, Wu Z, Zhao Q, Jiang X. Enhanced biodegradation of poorly available polycyclic aromatic hydrocarbons by easily available one. Int Biodeterior Biodegrad. 2013;84:72–8.
35. An X, Cheng Y, Miao L, Chen X, Zang H, Li C. Characterization and genome functional analysis of an efficient nitrile-degrading bacterium, Rhodococcus rhodochrous BX2, to lay the foundation for potential bioaugmentation for remediation of nitrile-contaminated environments. J Hazard Mater. 2020;389:121906.
36. Hou N, Zhang N, Jia T, Sun Y, Dai Y, Wang Q, Li D, Luo Z, Li C. Biodegradation of phenanthrene by biodemulsifier-producing strain Achromobacter sp. LH-1 and the study on its metabolisms and fermentation kinetics. Ecotox Environ Safe. 2018;163:205–14.
37. Chaineau CH, Rougeux G, Yepremian C, Oudot J. Effects of nutrient concentration on the biodegradation of crude oil and associated microbial populations in the soil. Soil Biol Biochem. 2005;37:1490–7.
38. Morris JJ, Lenski RE, Zinser ER. The Black Queen Hypothesis: evolution of dependencies through adaptive gene loss. MBio. 2012;3:203–16.
39. Huang ZJ, Zhu ZA, Wu XS, Lai XL, Wang PL, Hu XJ. Structural characteristics of King chard biochar and its mechanism of heavy metal adsorption. Environ Chem. 2016;35:766–72.
40. Khatami S, Deng Y, Tien M, Hatcher PG. Formation of Water-Soluble Organic Matter Through Fungal Degradation of Lignin. Org Geochem. 2019;135:64–70.
41. Xiao Z, Rasmann S, Yue L, Lian F, Zou H, Wang Z. The effect of biochar amendment on N-cycling genes in soils: A meta-analysis. Sci Total Environ. 2019;696:133984.
42. Braker G, Zhou J, Wu L, Devol AH, Tiedje JM. Nitrite reductase genes (nirK and nirS) as functional markers to investigate diversity of denitrifying bacteria in Pacific Northwest marine sediment communities. Appl Environ Microbiol. 2000;66:2096–104.
43. Kuypers MM, Marchant HK, Kartal B. The microbial nitrogen-cycling network. Nat Rev Microbiol. 2018;16:263–76.
44. Gul S, Whalen JK, Thomas BW, Sachdeva V, Deng H. Physico-chemical properties and microbial responses in biochar-amended soils: Mechanisms and future directions. Agric Ecosyst Environ. 2015;206:46–59.

45. Liu Q, Liu B, Zhang Y, Lin Z, Zhu T, Sun R, Wang X, Ma J, Bei Q, Liu G, Lin X, Xie Z. Can biochar alleviate soil compaction stress on wheat growth and mitigate soil N_2O emissions?. Soil Biol Biochem. 2017;104:8–17.
46. Zhang A, Cui L, Pan G, Li L, Hussain Q, Zhang X, Zheng J, Crowley D. Effect of biochar amendment on yield and methane and nitrous oxide emissions from a rice paddy from Tai Lake plain, China. Agric Ecosyst Environ. 2010;139:469–75.
47. Zumft WG. Cell biology and molecular basis of denitrification. Microbiol Mol Biol Rev. 1997;61:533–616.
48. Van ZL, Singh BP, Kimber SWL, Murphy DV, Macdonald LM, Rust J, Morris S. An incubation study investigating the mechanisms that impact N_2O flux from soil following biochar application. Agric Ecosyst Environ. 2014;191:53–62.
49. Tu Q, He Z, Wu L, Xue K, Xie G, Chain P, Reich PB, Hobbie SE, Zhou J. Metagenomic reconstruction of nitrogen cycling pathways in a CO_2-enriched grassland ecosystem. Soil Biol Biochem. 2017;106:99–108.
50. Sias SR, Stouthamer AH, Ingraham JL. The assimilatory and dissimilatory nitrate reductases of pseudomonas aeruginosa are encoded by different genes. Microbiology. 1980;118:229–34.
51. Gul S, Whalen JK. Biochemical cycling of nitrogen and phosphorus in biochar-amended soils. Soil Biol Biochem. 2016;103:1–15.
52. Sundareshwar PV, Morris JT, Pellechia PJ, Cohen HJ, Porter DE, Jones BC. Occurrence and ecological implications of pyrophosphate in estuaries. Limnol Oceanogr. 2001;46(6):1570–7.
53. Wang Y, Hu Y, Zhao X, Wang S, Xing G. Comparisons of biochar properties from wood material and crop residues at different temperatures and residence times. Energy Fuels. 2013;27(10):5890–9.
54. Torres IF, Bastida F, Hernández T, Bombach P, Richnow HH, García C. The role of lignin and cellulose in the carbon-cycling of degraded soils under semiarid climate and their relation to microbial biomass. Soil Biol Biochem. 2014;75:152–60.

Figures

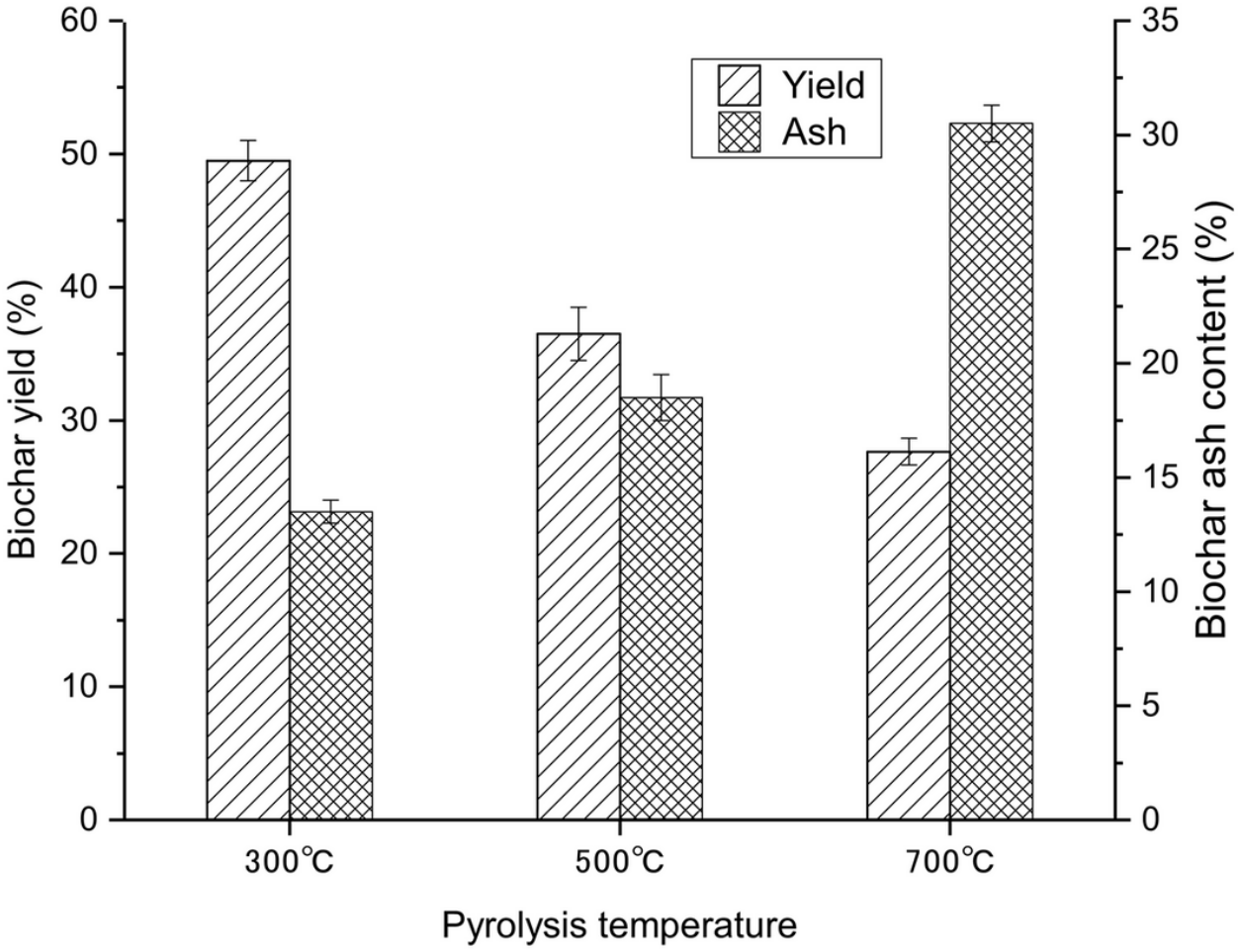

Figure 1

Yield and ash of biochars (BC300, BC500 and BC700). BC refers to the biochar obtained from rice straws; 300, 500 and 700 are the heating treatment temperatures. Error bars represent standard errors of the mean (n=3).

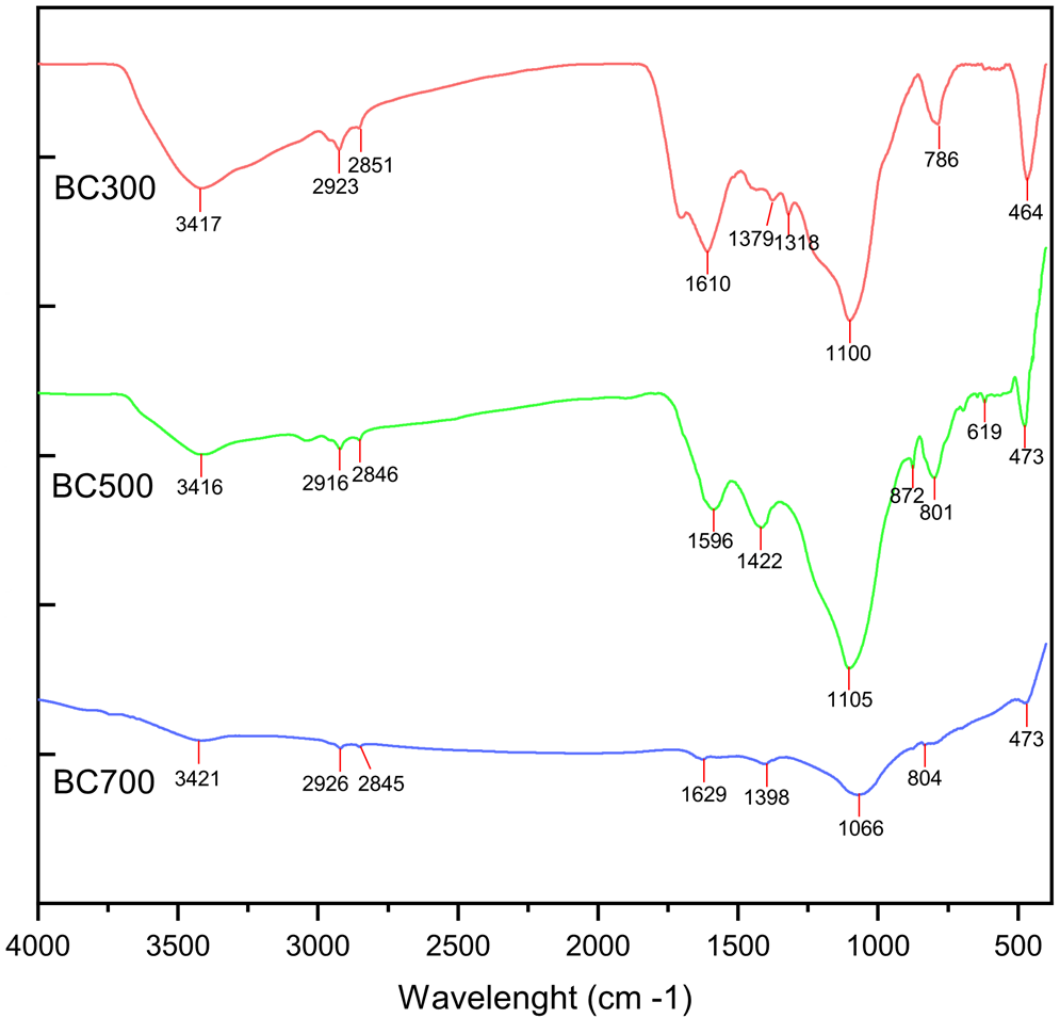

Figure 2

FTIR profiles of BC300, BC500 and BC700. BC refers to the biochar obtained from rice straws; 300, 500 and 700 are the heating treatment temperatures.

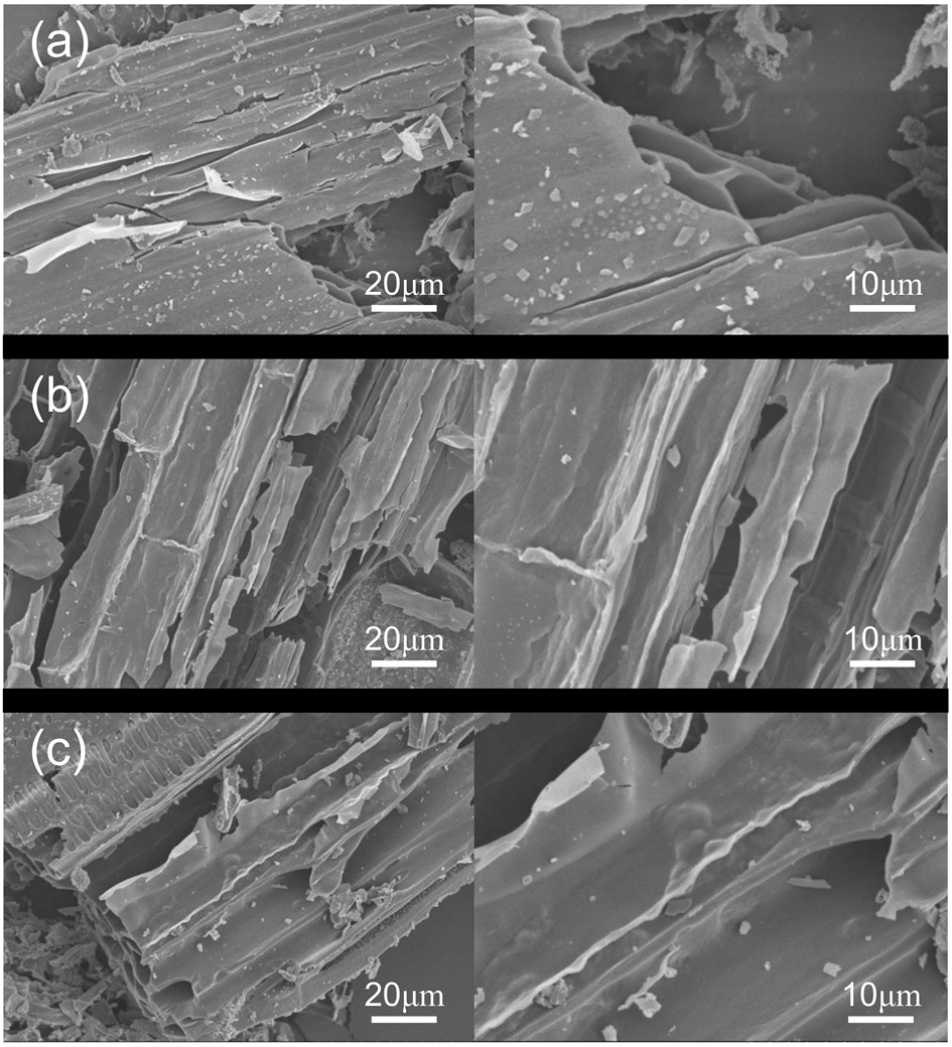

Figure 3

Scanning electron microscope (SEM) analysis of biochar. Scanning electron micrographs from (a) BC300, (b) BC500, and (c) BC700. Scale bar: 2k (left) and 5k (right). BC refers to the biochar obtained from rice straws; 300, 500 and 700 are the heating treatment temperatures.

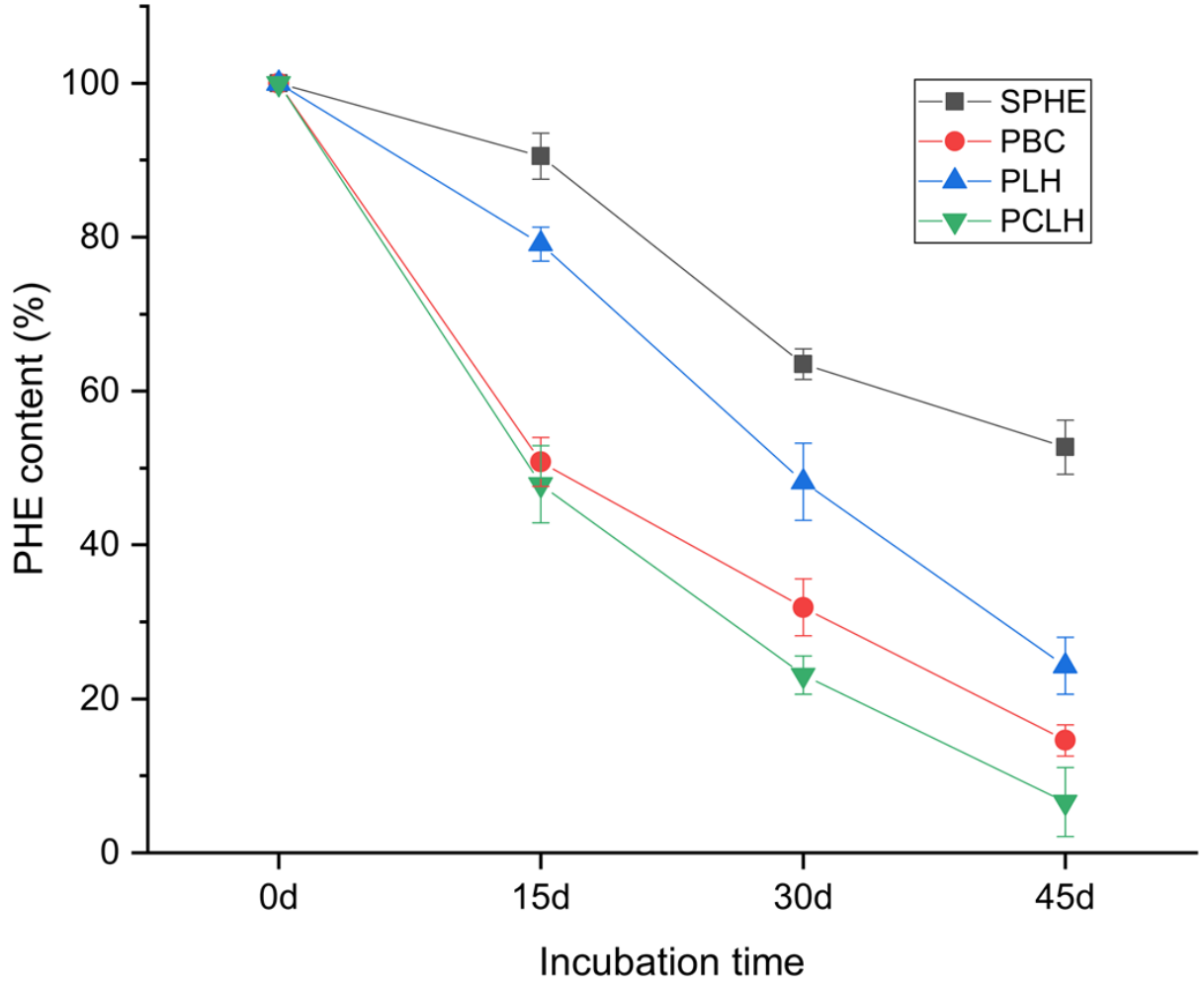

Figure 4

Residues of phenanthrene (PHE) in soil under the PBC (1% primary biochar + 300 mg/kg PHE), PLH (1% LH-1), PCLH (1% LH-1-composite), and SPHE (300 mg/kg PHE) treatments. Error bars represent standard errors of the mean (n=3).

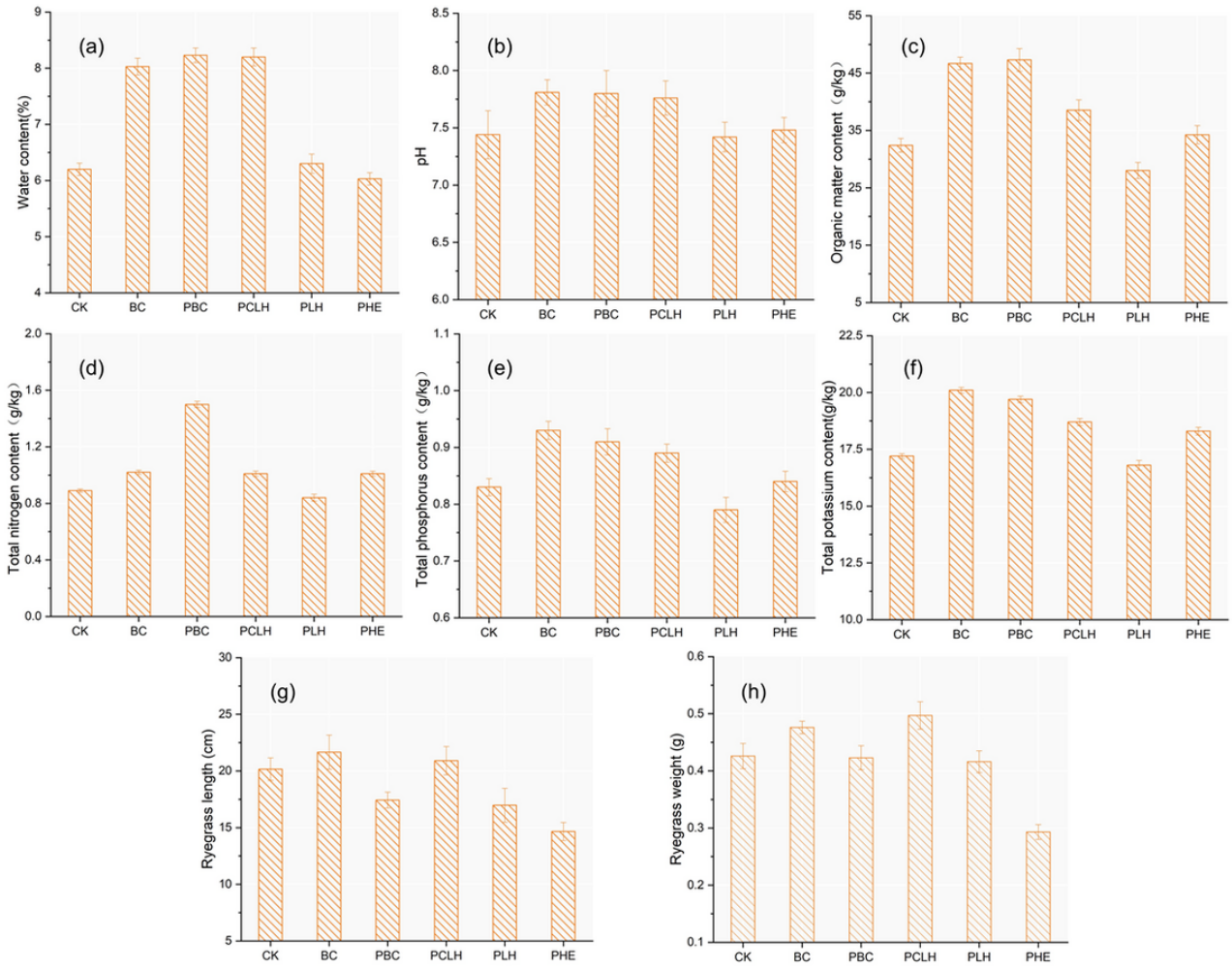

Figure 5

Different treatments effect on soil (a) water content, (b) pH, (c) organic matter content, (d) total nitrogen content, (e) total phosphorus content, (f) total potassium content, (g) ryegrass length, and (h) ryegrass weight. Physicochemical property of soil were significantly stimulated under biochar and microorganism treatments. Error bars represent standard errors of the mean (n=3).

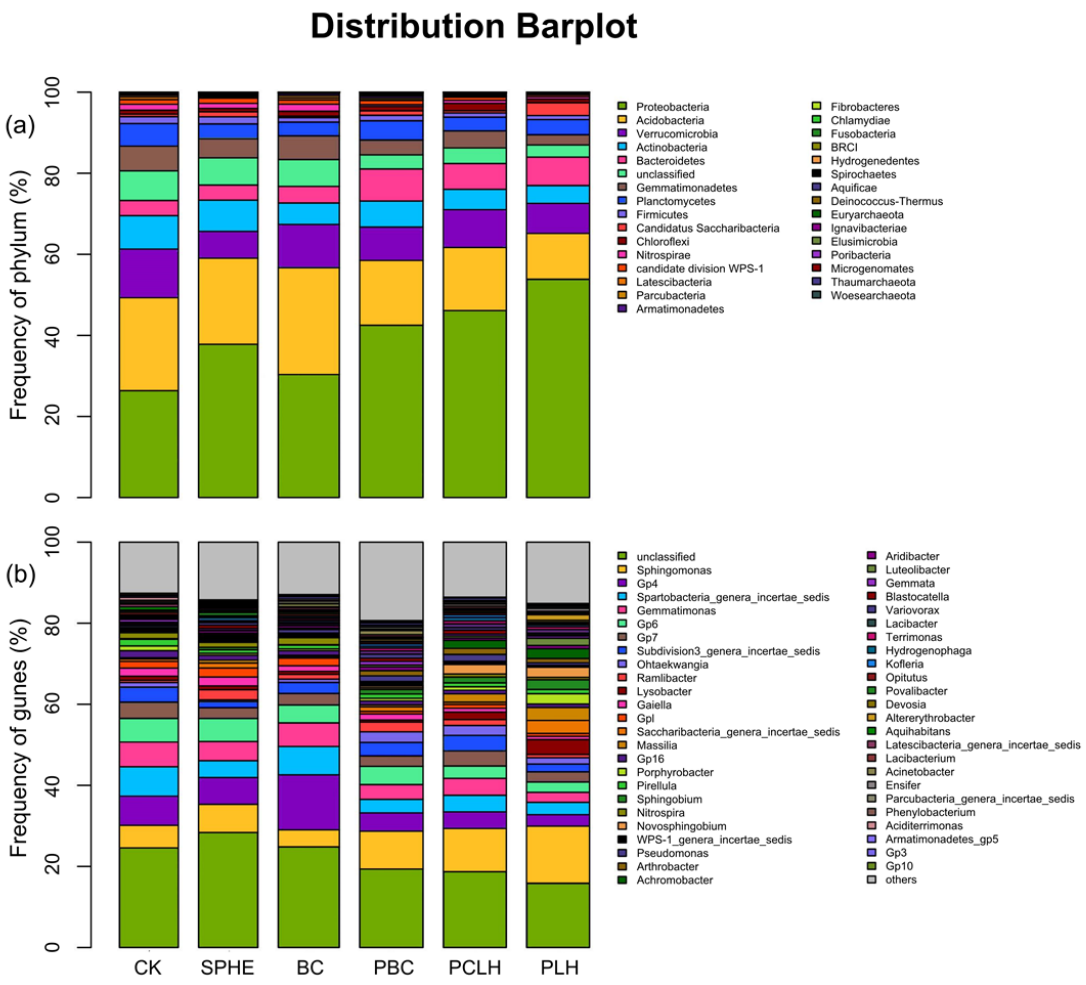

Figure 6

(a) Phylum-level microbial community structure species abundance. (b) Genera-level microbial community structure species abundance. The color corresponds to the name of each species under this taxonomic level, and the different color block widths indicate the relative abundance ratio of the different species.

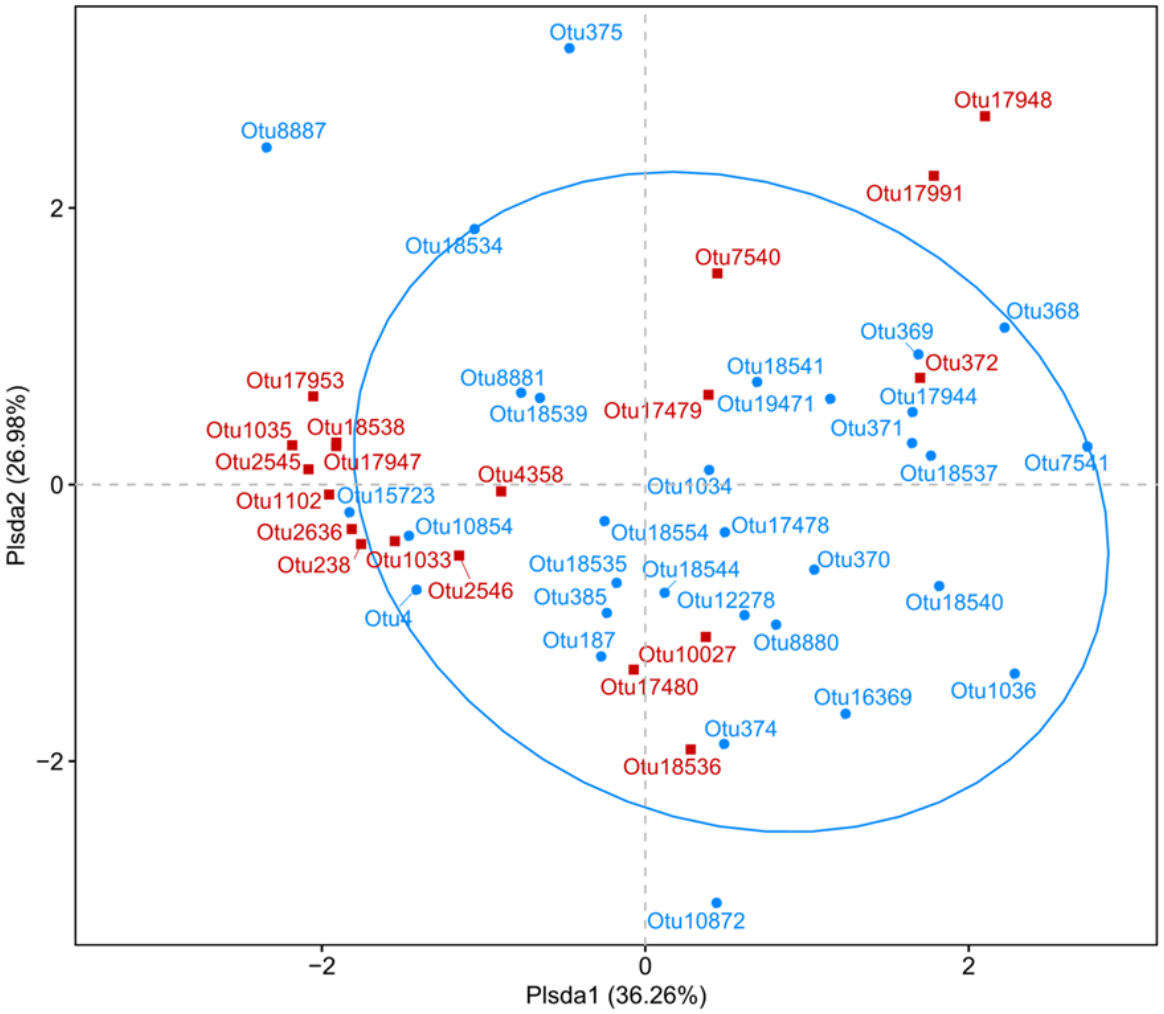

Figure 7

Principal coordinate analysis (PCoA) showing the correlations between (i) the abundance of the 100 first OTUs in terms of abundance in the 6 studied soils and (ii) the mean degradation efficiency (%90) of PHE.

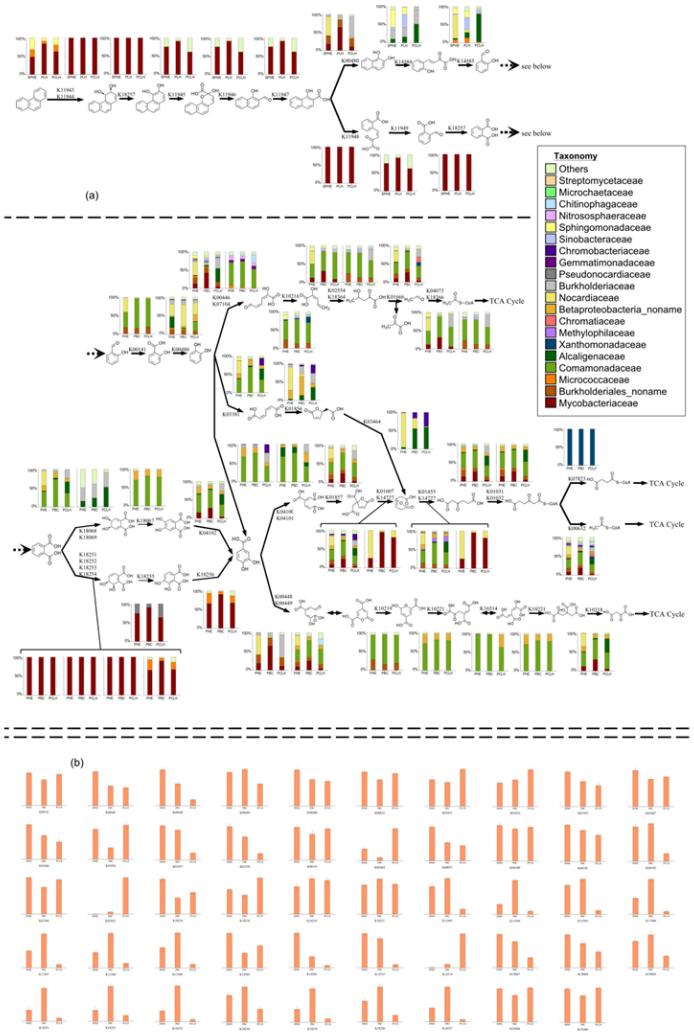

Figure 8

(a) Reconstruction of phenanthrene metabolic pathways. Black arrows are genes found in both metagenomes using GhostKOALA. The prefix R indicates enzyme-catalyzed reactions. The bar graph indicates the abundance of microorganisms within genes encoding PHE-degradation-related enzymes greater than 1%, and microorganisms with abundances less than 1% were represented by the others. (b) The histogram below represents the KO value of each enzyme involved in PHE degradation. Error bars represent standard errors of the mean.

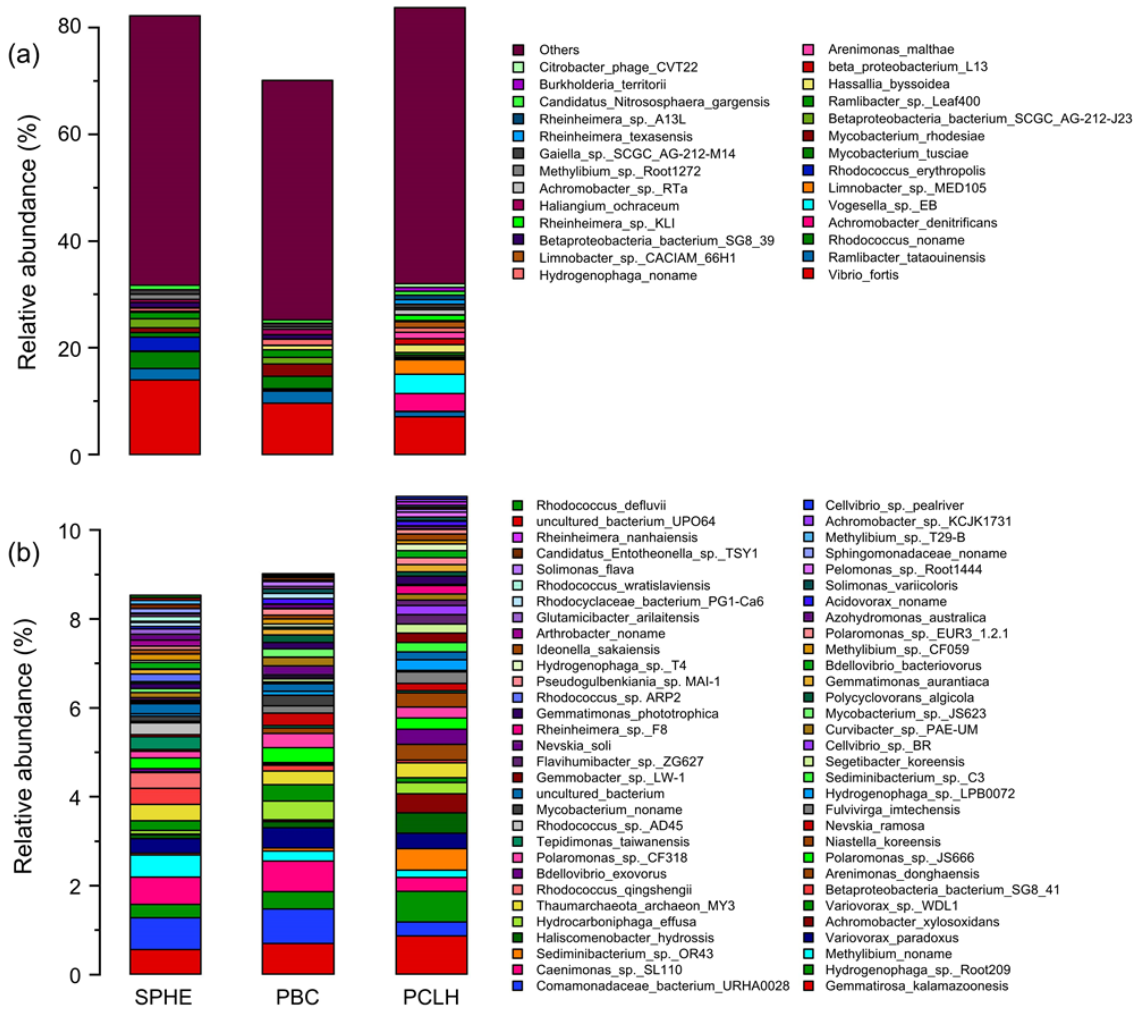

Figure 9

Relative abundance of species involved in PHE degradation. (a) Relative abundance of species with a relative abundance above 1% in soil. (b) Relative abundance of species that are related to PHE degradation in soil and whose relative abundance in the treatment group was more than 0.05% different from the control group.

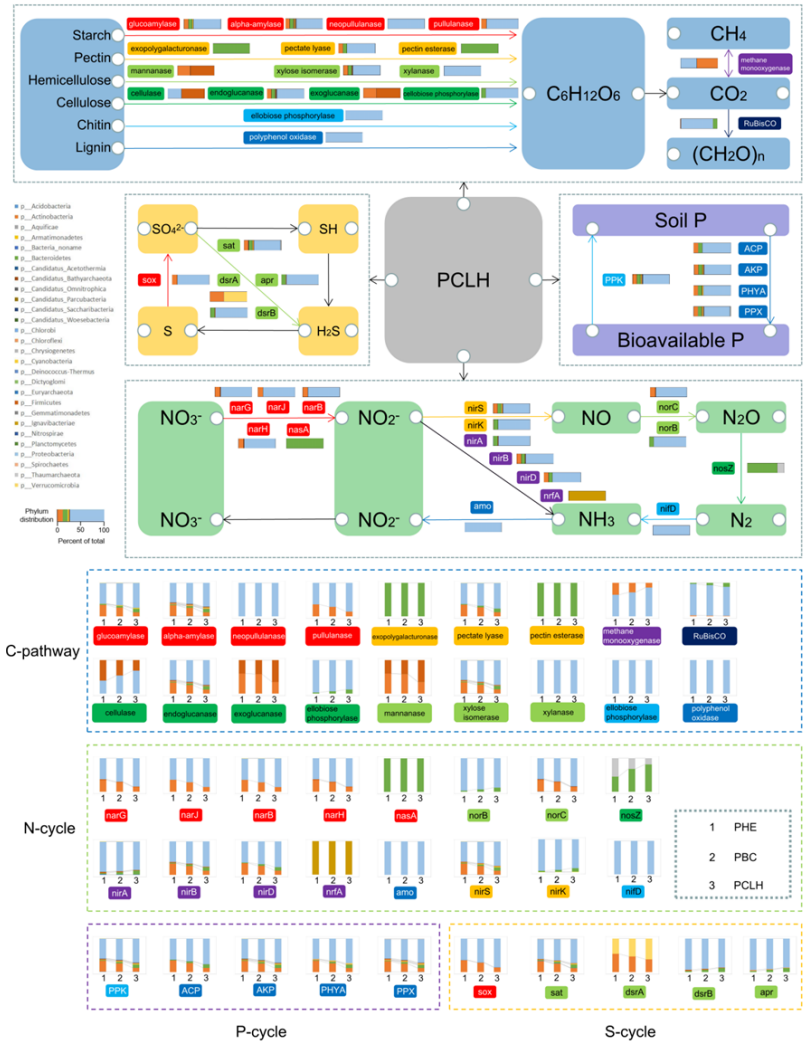

Figure 10

Predicted carbon, nitrogen, phosphorus and sulfur metabolic transformations. Predicted phylum-level genomic capacity for breakdown of small carbon-, nitrogen-, phosphorus- and sulfur-containing compounds. Bar plots indicate the fraction of genomes within a phylum encoding each function.

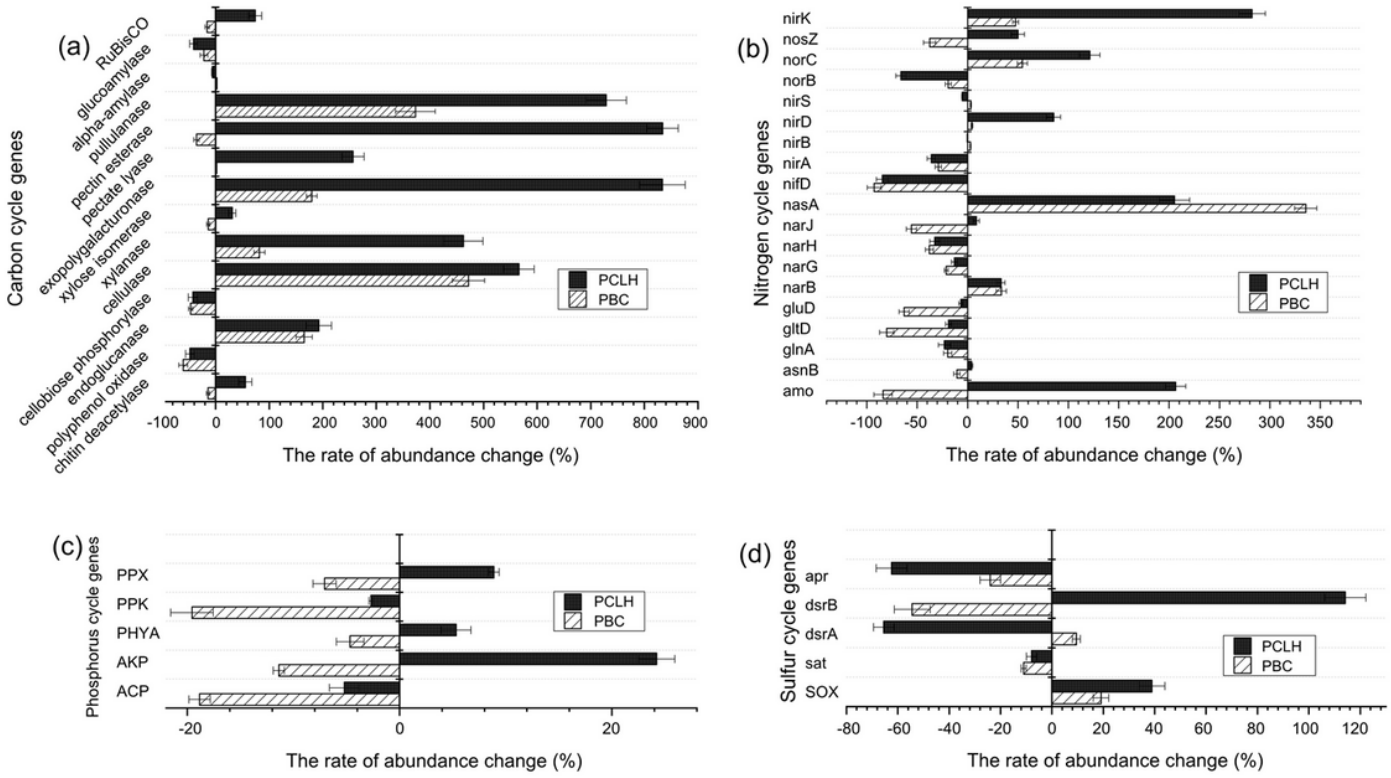

Figure 11

The changes in relative abundance of gene family-encoded enzymes involved in the carbon, nitrogen, phosphorus and sulfur cycles in different treatment groups. Error bars represent standard errors of the mean.